Mapping and ablation of atrial tachyarrhythmias : from signal to substrate

Groot, N.M.S. de

chapter 1

Introduction

Mapping of Atrial Tachyarrhythmias

Introduction

Tachyarrhythmias originating from the atria are common and give rise to a large number of visits to the primary care physician and even to hospital admissions.[1] Atrial tachyarrhythmias (AT) occur in subjects of all ages, though more frequently in the elderly.[1-4] They often arise in patients with ischaemic, hypertensive, valvular or congenital heart disease.[5-7] Although structural heart disease is present in many patients with AT, they also arise in patients with apparently normal hearts. [4]

Pharmacological therapy of AT is often not effective and catheter ablation may therefore be an attractive alternative treatment option because it is potentially curative.[7-11]

Associated with the on-going improvement in catheter ablation techniques, sophisticated mapping tools are being developed as well.[12-17] This allows more detailed mapping of AT which will increase our knowledge of the pathogenesis of AT.

AT are caused by disorders of impulse *formation* (automaticity, triggered activity) and/or disorders of *conduction* of electrical waves through the muscle structure of the atria (conduction block, reentry).[18] Several studies have demonstrated the role of atrial architecture in initiation and maintenance of AT.[19-23]

The aim of this chapter is to review mapping studies of AT – including (a) typical atrial flutter, atrial fibrillation and focal atrial tachycardias – and to discuss the relationship between atrial anatomy and pathogenesis of AT.

Atrial Tachyarrhythmias and Atrial Architecture

In case of a macro-reentry mechanism underlying the AT, large anatomical obstacles such as orifices of the pulmonary and caval veins or the atrioventricular valves may be delineating barriers of a reentry circuit around which the wavefront circulates. [24]

Not only macroscopic structures, but also the atrial microscopic structure is involved in pathogenesis of AT. Spach et al. were the first to provide evidence that '2-dimensional propagation is discontinuous in nature at a microscopic level' (Figure 1). [25-30]

In their experiments, variations in shape and amplitude of extracellular potential waveforms were studied when the direction of conduction was changed from longitudinal to transverse related to the fiber axis. They observed that in anisotropic myocardium, the shape of the upstroke of the transmembrane action potential depended on the direction of propagation in relation to the fiber orientation. Fast conduction in the longitudinal direction was associated with a slow upstroke and a long τ–foot and slow conduction in

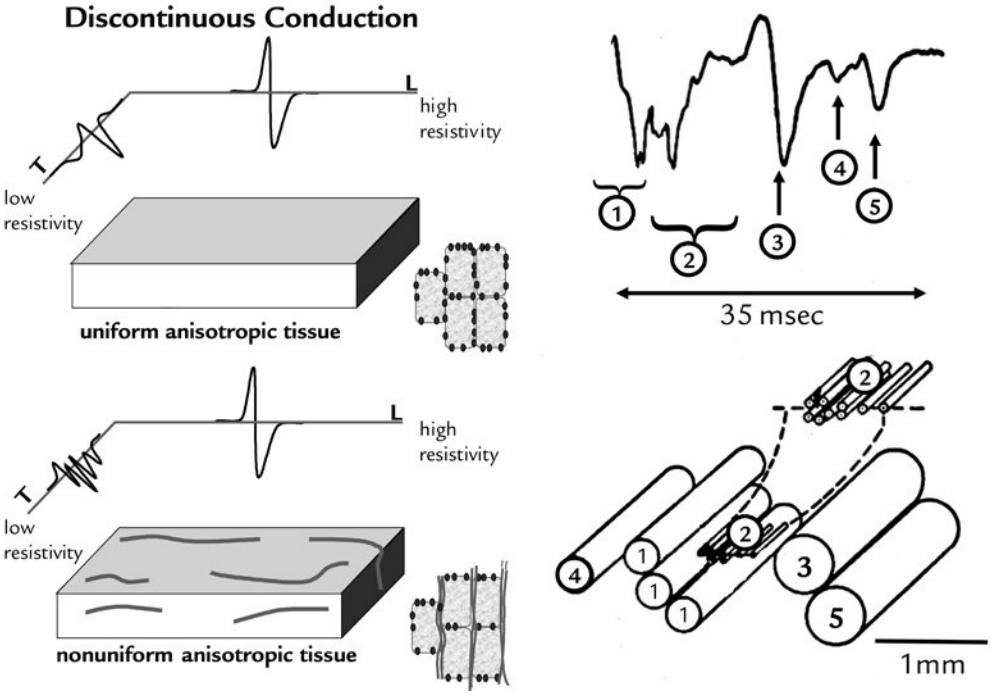

Figure 1.

Left panel: Electrograms recorded in the longitudinal and transversal conduction direction in relation to fiber orientation in uniform anisotropic and nonuniform anisotropic tissue. The electrogram in the transverse conduction direction in nonuniform anisotropic tissue consists of multiple deflections indicating discontinuous conduction.

Right panel: Discontinuous propagation at a microscopic level; fractionation of extracellular potentials due to electrical dissociation of muscle bundles (non-uniform anisotropy). Modified from Spach et al.[26]

the transverse direction with a fast upstroke and a short τ–foot. These direction depended differences were explained by the anisotropic distribution of intercellular connections (gap junctions).

Gap junctions along the fiber axis provide a low resistance to current flow which increases the space constant and hence the electrotonic current flow. Subsequently, the upstroke of the transmembrane potential in this direction decreases and the τ–foot increases. Due to high resistance barriers in the transverse direction, the space constant is reduced and the electrotonic current is therefore smaller. This results in an increase in the upstroke of the transmembrane potential and a decrease in the τ–foot. Consequently, as the safety factor is lower during longitudinal conduction than during transverse conduction, conduction block is more likely to occur during longitudinal conduction.

Discontinuous conduction can be the result of modifications of the atrial architecture including cell geometry (size and shape), gap junctions (distribution and conductivity) or the interstitial space (size and distribution). [31] It is likely that alterations of the atrial microscopic anatomy, caused by e.g. ageing and structural heart diseases, give rise to conduction abnormalities which in turn may facilitate genesis and perpetuation of tachyarrhythmias. [26;27]

The Right Atrium

The endocardial surface of the right atrium consist of muscle bundles of varying thickness, including the terminal crest, Eustachian ridge, the rim of the fossa ovalis, the pectinate muscles and the tricuspid vestibule.[32;33] Regional differences in thickness of the atrial wall affect conduction of electrical waves by giving rise to tissue anisotropy, modifying the wavefront curvature or by creating an electrical source-to-load mismatch. [20;29;34]

The terminal crest is involved in the pathogenesis of various forms of AT. It is a longitudinal muscular ridge which extends from the superior rim of the fossa ovalis in front of the superior caval vein downwards to the orifice of the inferior caval vein and forms the junction between the smooth walled (sinus venarum) and trabeculated part of the right atrium. The terminal crest gives rise over the entire length to 15- 20 smaller muscular trabeculations (the pectinate muscles, **Figure 2**). Even in normal hearts, conduction along the terminal crest is anisotropic in nature (fast conduction in the longitudinal direction and slow conduction in the transverse direction) which is due to a sparse lateral cell-to-cell coupling. [35] Histological studies of the atria obtained from subjects without AT revealed that there is a disorganized arrangement of muscle fibers at the junction between the terminal crest and the pectinate muscles and at the site of the terminal ramifications of the terminal crest (cavo-tricuspid isthmus). [21] The multi-directional orientation of muscle fibers at these sites also varies considerably between subjects. Hence, the complex atrial architecture of the terminal crest may facilitate abnormalities in conduction and thereby provide an arrhythmogenic substrate.

In patients without structural heart disease, focal atrial tachycardias are often found to

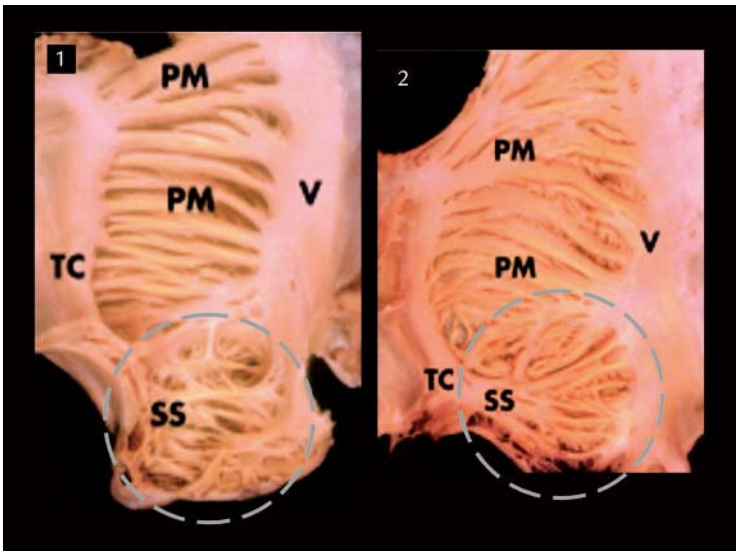

Figure 2.
Endocardial aspect of the right atrium of 2 humans without a history of AT. There is variation in atrial architecture, particularly in the terminal ramifications of the chest.
TC: terminal crest, PM: pectinate muscles, SS: septum spurium and V: vestibule.

originate from the terminal crest. [36] This could be attributed to the presence of cells with automatic properties combined with myocytes with sparse lateral coupling as areas with focal activity embedded within tissue with poor cell-to-cell coupling facilitate the arisal of focal atrial tachycardias. [37-39] During typical atrial flutter, the terminal crest forms a functional barrier of the reentry circuit. [40] In some patients, gaps in this barrier result in a reentrant tachycardia confined to the upper part of the right atrium which can be terminated by elimination of conduction through the crista. [41]
Optical mapping studies in isolated sheep heart during atrial fibrillation demonstrated that lines of conduction block corresponded with the location of the pectinate muscles. [42] In addition, they observed that epicardial breakthroughs were the consequence of transmural conduction or the result of reentry through pectinate muscle bundles connected to the epicardium. It is most likely that in the human atria conduction may occur also transmurally.

The Left Atrium: the pulmonary veins
Ever since the discovery that ectopic beats originating from the pulmonary veins may trigger atrial fibrillation (AF), anatomy of the pulmonary veins has become a major topic of interest (**Figure 3**). Macroscopic studies, histological examination and various imaging modalities such as pulmonary vein angiography, contrast-enhanced computed tomography and magnetic resonance imaging have all demonstrated that human pulmonary vein

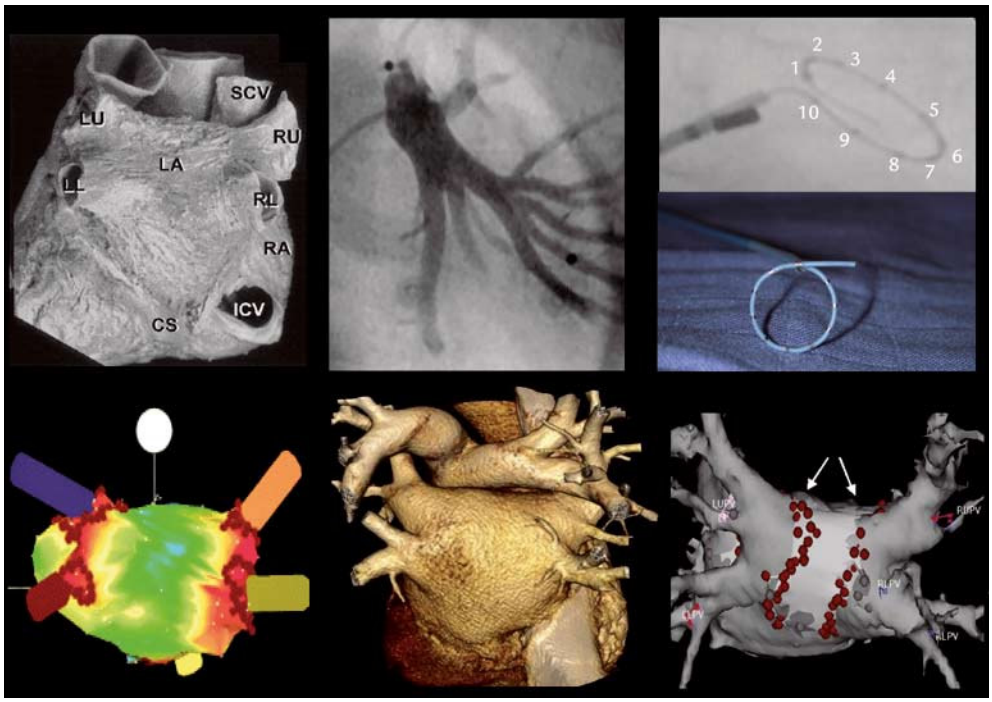

Figure 3.
Upper left panel: normal heart demonstrating four pulmonary veins.
RA: right atrium, LA: left atrium, SCV: superior caval vein, ICV: inferior caval vein, CS: coronary sinus, RU and RL: right upper and lower pulmonary vein, LU and LL: left upper and lower pulmonary vein.
Upper middle panel: angiography of the left inferior pulmonary vein.
Upper right panel: example of an ablation catheter designed for pulmonary vein ablation.
Lower left panel: 3-dimensional reconstruction of the pulmonary veins. The ablation lesions encircling the ostia are represented by red markers.
Lower middle and right panel: CT reconstructions of the pulmonary veins.

anatomy (e.g. the number and dimensions of pulmonary veins, distinct ostia or common trunks) is highly variable. [43-48]

In order to comprehend the role of the pulmonary veins in the pathogenesis of AT, histological and electrophysiological characteristics of myocardial sleeves extending from the left atrial myocardium (13-25 mm) onto the pulmonary veins were studied in detail.[40;43;44;46;47;49] These myocardial sleeves are located on the epicardial side of the veins and are separated from the smooth muscle media of the vein by fibro-fatty tissue. Going from proximal to distal in the pulmonary veins, thickness of the sleeves decreases and distally they may even be composed of isolated fascicles only. [50] The length of the sleeves in the superior pulmonary veins is longer than in the inferior pulmonary veins and the longest sleeves are often found in the left superior pulmonary veins. [46;50] Pulmonary veins can also be connected to each other by intermingling of their myocardial sleeves. Histological examination revealed that the arrangement of myocytes of these sleeves is disorganized

and that the myocardium contain gaps consisting of areas of fibrotic tissue. At the ostial junction, the sleeve is composed of multiple layers myocardium with different spatial orientations. This complex fiber arrangement results in non-uniform anisotropic conduction which may facilitate reentry. Hocine et al. indeed demonstrated that in canine atria sudden changes in fiber orientation within the pulmonary veins were related to zones of conduction delay.[49] Similar findings were reported by Hamabe et al. [51] They showed that at the junction between the left atrium and the pulmonary veins gaps of connective tissue gave rise to marked conduction delay which were mainly present during pacing from the distal pulmonary veins but not during sinus rhythm.

Histological examination of the pulmonary vein sleeves revealed the presence of different population of myocardial cells. [52] This might explain variation in duration of action potentials measured from pulmonary vein myocytes and the resulting regional differences in refractoriness contributing to initiation and/or perpetuation of AT. [53]

Other investigators have provided evidence that abnormal automaticity or triggered activity are responsible for arrhythmogenicity of the pulmonary veins. [54] Ectopic foci are usually found at 2 to 4 cm within the pulmonary vein. Perez-Lugones et al. demonstrated that there are cells (P cells, transitional cells and Purkinje cells) within the myocardial sleeves with specialized conduction properties and the presence of such cells might account for pulmonary vein automaticity. [44]

InterAtrial Connections: Bachmann's Bundle

Bachmann's bundle is a band of muscle fibers extending from the junction between the right atrium and superior caval vein towards the left atrial appendage where it divides in two branches (upper panel **Figure 4**).[19;55;56] The upper branch continues from the left atrial appendage in front of the orifices of the left pulmonary veins towards the left atrial free wall. The lower branch extends from the base of the left atrial appendage towards the mitral ring. These two branches intermingle on the lateral free wall of the left atrium and continue as a thin branch in the interatrial groove.

Experimental and clinical studies have provided evidence that wavefronts propagating from the left to the right atrium and vice versa via Bachmann's bundle may play an important role in the pathogenesis of AF.[19;55;57;58]

Indirect, endocardial mapping studies comparing conduction across Bachmann's bundle in subjects without AT and patients with persistent or permanent AF demonstrated that conduction abnormalities were most pronounced in patients with AF, particularly in patients with permanent AF. [58] Isolation of the pulmonary veins is less effective in humans with conduction abnormalities at Bachmann's bundle. [58]

During induced AF in dogs with sterile pericarditis, bachmann's bundle was essential for formation of multiple unstable reentry circuits perpetuating AF. [57] Consequently, ablation of Bachmann's bundle terminated AF. [55]

Conduction abnormalities at Bachmann's bundle may be caused by histopathological

Bachmann's Bundle

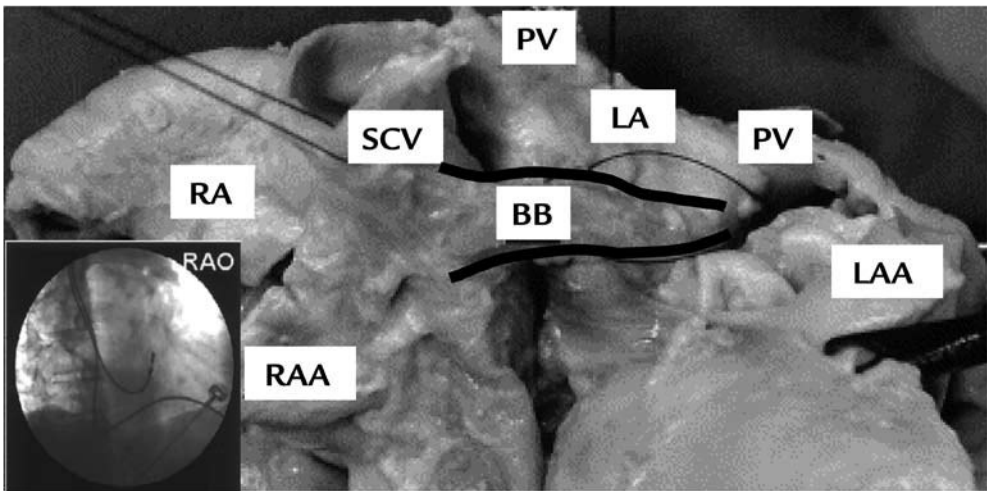

Coronary Sinus

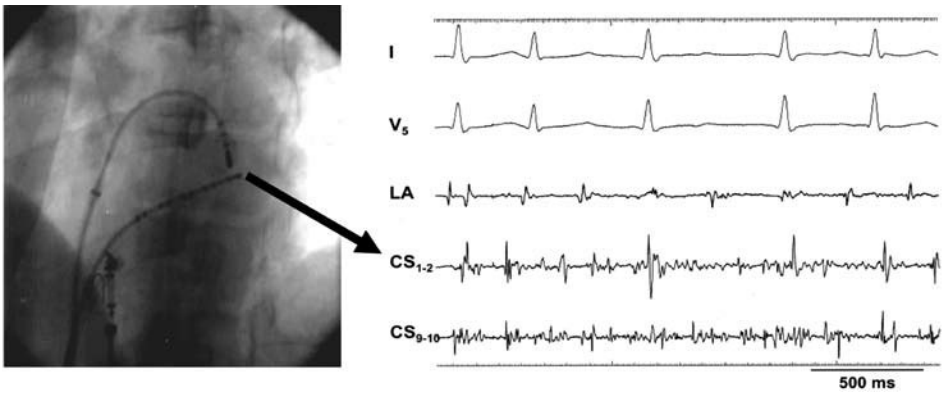

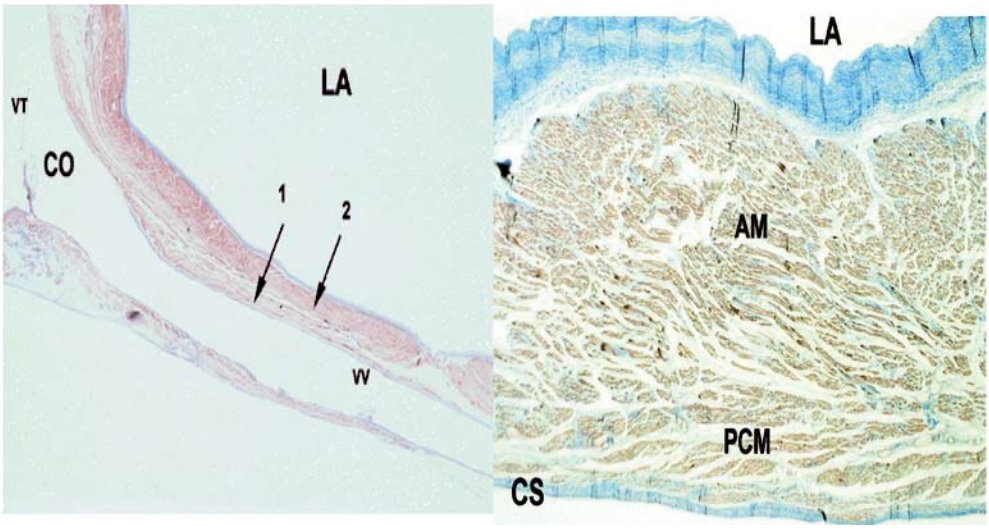

Figure 4.
Upper panel: anterosuperior view of the heart demonstrating the position of bachmann's bundle. The fluoroscopic image in the lower left corner shows a pacing lead positioned at bachmann's bundle (right anterior oblique view). Modified from Lemery and Khaja et al.[19;56]
Middle panel: mapping catheter positioned within the coronary sinus records rapid electrical activity during AF.
Lower left panel: longitudinal section through the coronary sinus. The striated myocardium of the coronary sinus (arrow 1) can be distinguished from left atrial myocardium (arrow 2).
CO: coronary sinus ostium, VV: valve of Vieussens, VT: valve of Thebesius.
Lower right panel: transverse section through the coronary sinus again demonstrating merging of coronary sinus myocardium (PCM) and left atrial myocardium (AM). Modified from Oral, Chauvin et al.[60;62]

alterations. Becker et al. performed microscopic studies of bachmann's bundle obtained from humans with a history of paroxysmal AF (n = 10, coronary artery disease: n = 5, mitral valve disease n = 2, and coronary artery/mitral valve disease: n = 3) and from humans without a history of AF (n = 10, coronary artery disease: n = 5, coronary artery/mitral valve disease: n = 1, left ventricular hypertrophy: n = 2, no structural heart disease: n = 2).[59] Fibro-fatty replacement with a patchy distribution was found in all patients but it was more pronounced in patients with AF. Interestingly, atrial myocardial micro-infarction was observed in two AF patients.

InterAtrial Connections: Coronary Sinus

Another essential interatrial connection which may serve as a preferential conduction route is the coronary sinus myocardium. The coronary sinus is a large venous structure that extends from the oblique vein of Marshall to the right atrium and is surrounded by a cuff of striated muscular fibres (25-51 mm in length). Numerous fibers emerge from this cuff and are attached to the left atrial wall, including the Marshall muscle bundle. [60]

The existence of these musculature connections can be explained by the embryological origin of the coronary sinus musculature and the left atrium. [60] During fetal development, the primitive atria are separated from the sinus venosus. The left horn of the sinus venosus gives rise to the coronary sinus and the primitive atrium to a narrow muscular band around the mitral annulus. Connections between the sinus venosus and adjacent atrium bordering the mitral annulus may be maintained throughout development in order to form the connective muscle bundles.

Experimental and clinical studies have shown that the coronary sinus musculature plays a role in both initiation and maintenance of various tachyarrhythmias (middle and lower panel **Figure 4**). [23;58;61-64] Focal atrial tachycardias and AF due to automaticity or triggered activity have been reported to originate from the coronary sinus musculature. [23;63] In patients with chronic AF and rheumatic heart disease, episodes of induced AF started by a rapid organized AT originating from the coronary sinus os and ablation at this site eliminated AF. [61] Comparing conduction through coronary sinus musculature in subjects without AT and patients with persistent or permanent AF, conduction abnormalities were most pronounced in patients with permanent AF. [58]

Mapping studies have also revealed that the coronary sinus myocardium can be 1) a part of the reentry circuit in case of atypical flutter, 2) the slow pathway of an atrioventricular nodal reentry tachycardia and 3) the atrial connection of epicardial posteroseptal accessory pathways in patients with atrio-ventricular reentry tachycardias. [64]

Atrial Fibrillation and Fibrosis

Augmentation of fibrosis or changes in the expression of gap junctional proteins giving rise to tissue anisotropy has been suggested as "the second factor" contributing to persistence of AF. Alterations in myocardial structure have been reported in patients with AF, including focal degeneration, necrosis, fibrosis or fibro-fatty myocardial replacement and changes in the arrangement and number of gap junctions. [65] Fibrosis and redistribution of gap junctional proteins are also age-dependent phenomena and this may explain the higher incidence of AF in elderly patients. [28;65-67]

Fibrosis is defined as an excessive deposition of extra-cellular matrix which mainly consists of collagen type I, III and the cross linking glycoprotein fibronectin. Several studies have demonstrated that AF is associated with augmentation of fibrosis. [59;66;68;69]

Boldt et al. analysed tissue samples from the left atrial free wall obtained from patients with lone AF, AF and mitral valve disease and patients in sinus rhythm with or without mitral valve disease. [68] In the AF patients, thick connective tissue fibers were interpositioned between muscle bundles and between cardiomyocytes whereas in the sinus rhythm patients only a fine network of collagen was present between the separate muscle bundles and there was no connective tissue between cardiomyocytes. Comparing the AF and sinus rhythm group, there was a higher content of collagen I, III and fibronectin in all AF patients thereby demonstrating a relation between AF and fibrosis. Comparing patients with and without mitral valve disease, either during AF or sinus rhythm, there was no difference in the content of collagen type I or fibronectin. However, there was a significant increase in collagen type III in patients with mitral valve disease. This finding is consistent with an experimental study which demonstrated that in case of mechanical stretch fibroblasts respond with an increase in collagen type III mRNA whereas collagen type I mRNA production remains unaltered. [65;70]

Corradi et al. demonstrated that there were regional differences in the degree of interstitial remodeling in the left atrium in patients with mitral valve disease. [69] Tissue samples were taken off the left atrial free wall and the left atrial appendage from patients with chronic AF and mitral valve disease including mitral stenosis (9), mitral insufficiency (13) and both mitral stenosis and mitral insufficiency (11). The degree of interstitial fibrosis and perivascular fibrosis was determined and compared with tissue samples from control patients without structural heart disease or atrial arrhythmias. In the patients with mitral valve disease, interstitial fibrosis was more pronounced in the left atrial free wall than in the left atrial appendage. No such differences were found in the control group. A higher degree of interstitial fibrosis at the left atrial appendage was associated with a higher de-

gree of interstitial fibrosis at the left atrial free wall. The degree of perivascular fibrosis in patients with mitral valve disease was comparable with the control patients. Also, there were no differences between the samples obtained from the left atrial free wall and the left atrial appendage in both control and mitral valve disease patients.

There was no relation between interstitial or perivascular fibrosis and age or AF duration. Recurrences of AF after ablation were associated with augmentation of interstitial fibrosis. These findings thus indicate the importance of fibrosis in the pathogenesis of AF. Fibrosis results in side-to-side decoupling of atrial myocytes causing slowing of conduction. [27] If electrical conduction disturbances form the substrate of AF, regions of local heterogeneity in conduction may be amenable for ablation.

In order to comprehend the relation between atrial structure and the mechanism of AT, a spatial model of the excitation sequence plotted on a reconstruction of the atria may be helpful. For this purpose, various cardiac mapping techniques have been developed.

Cardiac Mapping

Cardiac mapping is defined as a method by which potentials recorded directly from the surface of the heart are spatially depicted as a function of time in an integrated manner. [71] Isochronal or activation mapping is the most commonly used cardiac mapping approach. An isochronal or activation map provides a spatial model of the excitation sequence and its construction requires detection of the local activation time of the myocardium surrounding the recording electrode (**Figure 5**). The objective of cardiac mapping in general is to increase our knowledge of arrhythmogenesis and to guide therapy of tachyarrhythmias.

Mapping Techniques

In recent years, a number of different cardiac mapping techniques has been introduced.[12-15;72-74] Mapping devices record cardiac potentials by electrodes which are in close contact with the surface of the heart or they reconstruct cardiac potentials from cavitary potentials measured by electrodes which are not in contact with myocardial tissue.[12;13;15;72] The simplest mode of endocardial mapping applied in clinical practice is fluoroscopy-based multi-electrode catheter mapping (e.g. Halo catheter, **Figure 6**). These catheters record

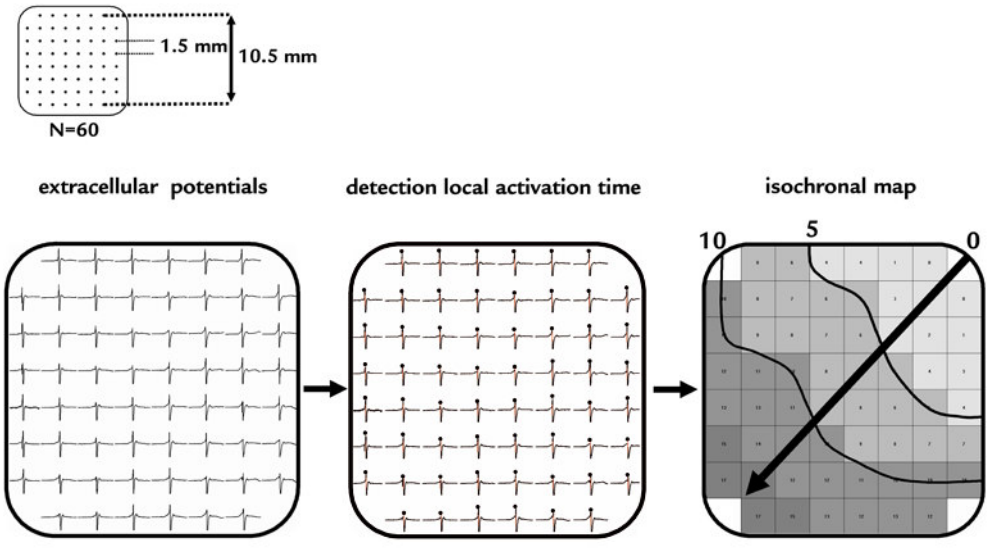

Figure 5.

Example of a construction of an isochronal map with an epicardial template containing 60 unipolar electrodes with an inter-electrode distance of 1.5 mm. The local activation time at each electrode is determined by marking the intrinsic deflection of the extra-cellular potential (black dot). Isochrones are lines connecting points in the mapping area with equal activation times. The arrow indicates the propagation direction of the activation wavefront across the mapping area.

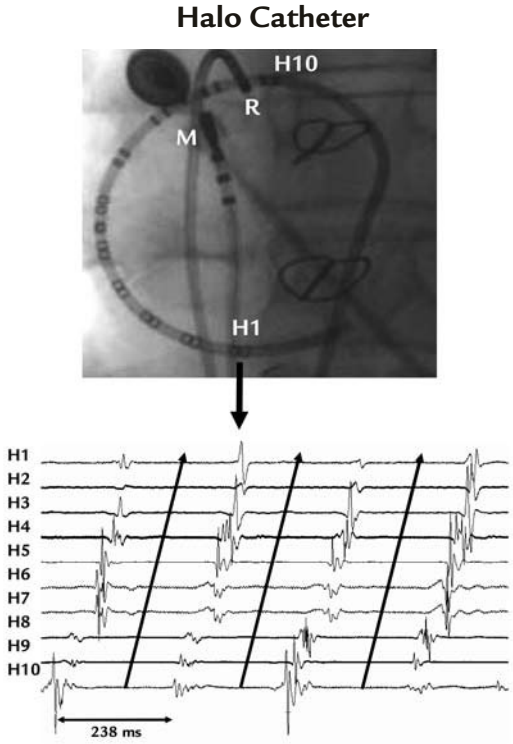

Figure 6.
Fluoroscopy-based multi-electrode catheter mapping using a Halo-catheter.
Upper panel: a Halo catheter (H) is positioned in the right atrium. The shaft of this catheter contains 10 bipolar electrodes (H1-H10). The corresponding recordings shown in the lower panel demonstrate a counterclockwise atrial flutter.
M = mapping catheter, R = right atrial reference catheter, positioned in the right atrial appendage.

electrograms simultaneously from multiple endocardial sites and the location of the recording sites can only be estimated by fluoroscopy.[14;75;76]
Sequential mapping, either single- or multi-site mapping, is only reliable when the activation sequences are reproducible. It requires a mental reconstruction of the activation sequence and this may be difficult in case of complex arrhythmias such as late post-operative atrial tachycardias in patients with surgically corrected congenital heart disease.
Several sophisticated endocardial sequential mapping systems have nowadays overcome this limitation by creating a 3-dimensional reconstruction of the activation sequence. Well-known examples of such mapping techniques include LocaLisa and the 3-dimensional electro-anatomical mapping system (CARTO™).[12;13;16;17;72] The basic principles of the CARTO™ system are summarized in **Figure 7**. This mapping technique is however still time consuming when high density activation maps are required to localize target sites for ablation. A mapping technique which allows fast and accurate identification of the area of interest may therefore be advantageous, particularly in patients with hemody-

namically unstable tachycardias. To overcome this limitation, a new mapping technique – Qwik-mapping – was recently introduced. This mapping approach is an extension of the CARTO™ system and allows construction of activation maps using both contact and cavitary potentials (**Figure 8**). Qwik mapping accelerates construction of activation maps as cavitary potentials are recorded by multiple electrodes in the catheter's shaft during acquisition of contact potentials and during navigation of the mapping catheter. Hence, selection of target sites for ablation is facilitated as less contact potentials are required to quickly identify the area of interest.

A limitation of endocardial mapping is the uncertainty of good contact between the mapping electrode and atrial tissue. Also, some atrial regions such as Bachmann's bundle,

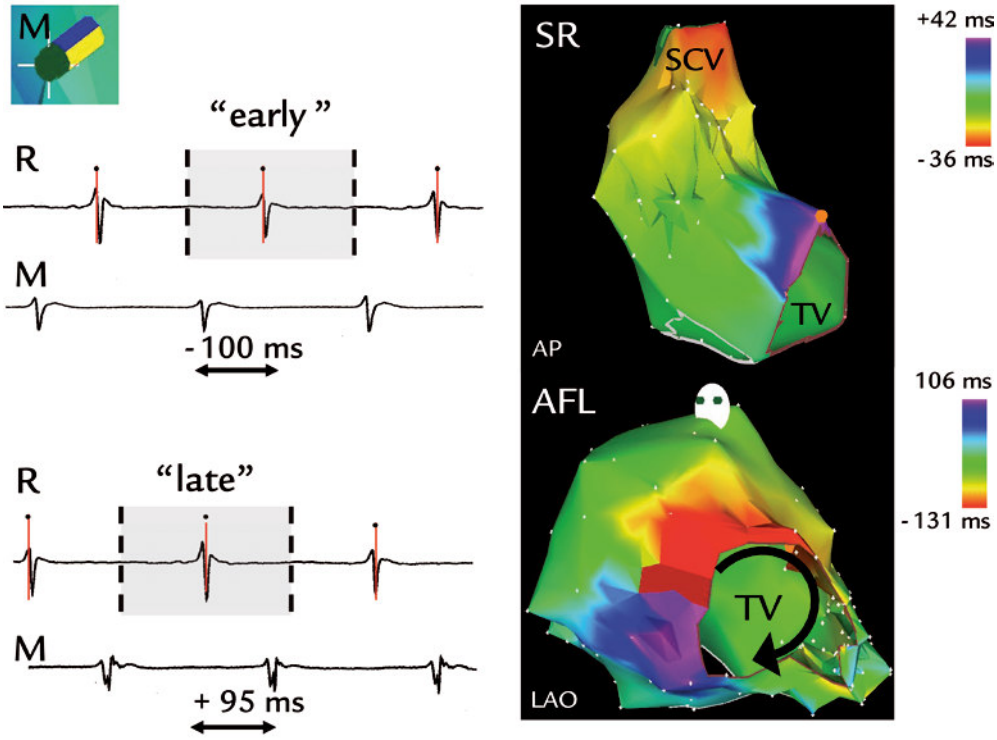

Figure 7.

Basic principles of the CARTO™ system. Left panel: The position and orientation of the tip of the mapping catheter (M) is continuously displayed by an icon on the screen. The relative activation time of each recorded potential is determined in relation to a fixed point of a reference electrogram (R) and used to create a color coded activation map.

Right panel: color coded 3-dimensional activation map of the right atrium constructed during sinus rhythm (SR) and atrial flutter (AFL).

AP = antero-posterior view, LAO = left anterior-oblique view.

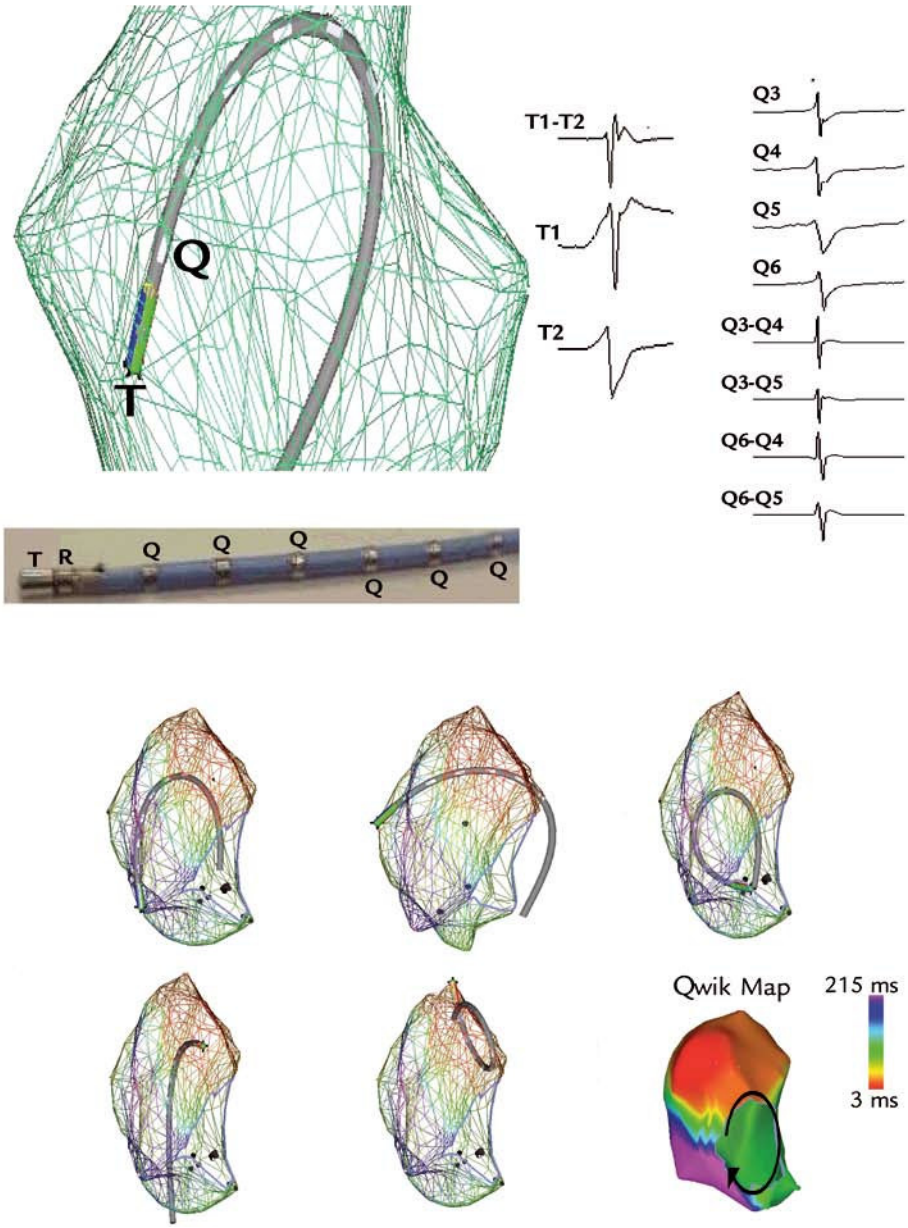

Figure 8.

Principles of Qwik-mapping. *Upper panel:* The shaft of the mapping catheter contains a 4 mm tip and ring electrode and 6 rows of 4 orthogonal electrodes. Contact potentials are collected by single point-to-point mapping. During acquisition of these contact potentials, cavitary potentials (Qwik points) are recorded by the shaft electrodes. In addition, contact potentials are recorded during manoeuvring of the catheter.
Lower panel: Construction of a Qwikmap of the right atrium during atrial flutter (CL = 220 ms). Only five contact points were used for creation of this activation map. The position of the QwikMap™ catheter at each of these point is shown. By positioning and rotating the catheter in a loop, numerous non-contact points were collected.

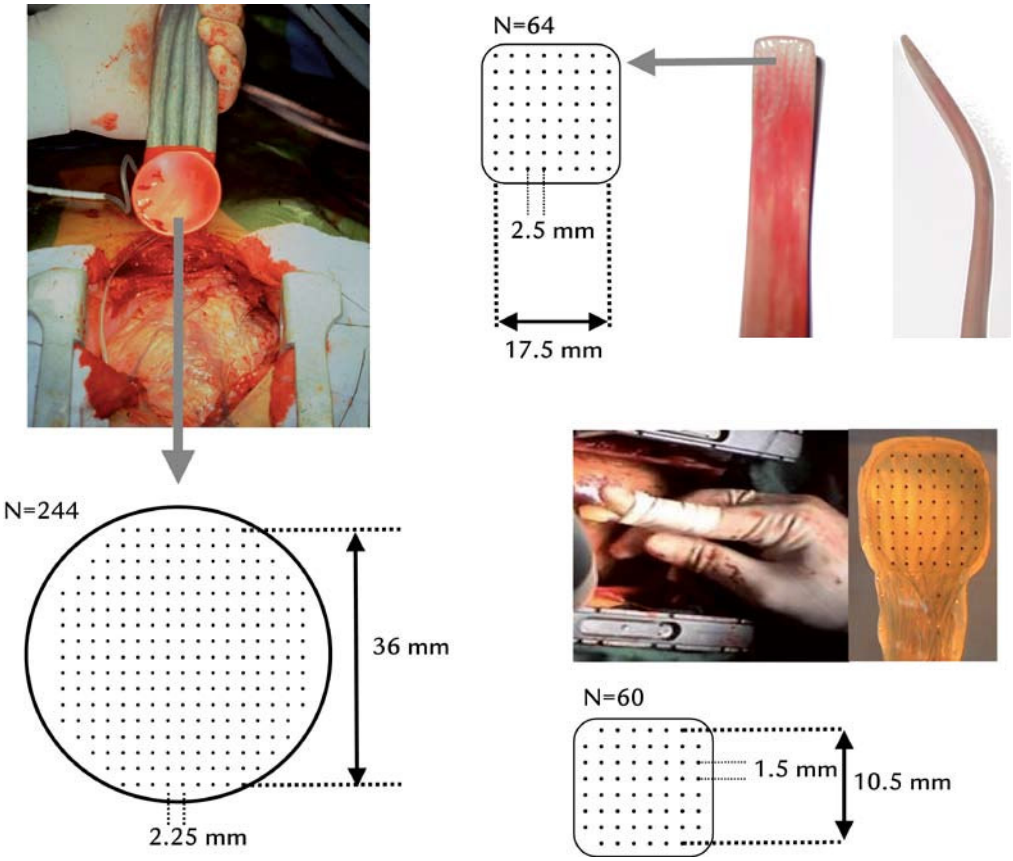

Figure 9.
Epicardial mapping devices used for mapping of the atria during cardiac surgery.
Left panel: mapping of the right atrial free wall, right atrial appendage and right atrial posterior wall was performed with a spoon shaped mapping electrode. This electrode contains 244 unipolar electrodes with an inter-electrode distance of 2.25 mm and covers an area of 36x36 mm. *Upper right panel:* for mapping of the left atrial posterior wall, a rectangular electrode was used (inter-electrode distance of 2.5 mm, mapping area: 17.5 mm). *Lower right panel:* mapping of multiple sites of the entire right and left atrium was performed with a 1 cm^2 electrode containing 60 unipolar electrodes with an inter-electrode distance of 1.5 mm.

can not be reached by endocardial mapping. Open chest surgery offers the opportunity to perform epicardial mapping. Epicardial mapping studies during open chest surgery are usually performed with hand-made multi-electrode arrays. Examples of epicardial multi-electrode templates are demonstrated in Figure 9.

Extracellular Potentials

A main element in cardiac mapping is correct interpretation of the morphology of extracellular potentials. Extracellular potentials features are used to detect the local activation time of atrial tissue surrounding the recording electrode. In case of an unipolar

electrogram, the maximum negative slope can be used to determine the moment of local activation as it coincides with the moment of maximum rate of rise of the trans-membrane potential (time differences less than 50 μs). [26] In turn, the maximum rate of rise of the transmembrane potential correspond with the maximum increase in sodium current and its conductance. [77] Determination of the local activation time using bipolar electrograms is more complicated. As a bipolar electrogram represents the difference between two unipolar electrograms, the local activation time is also the difference of the local activation time of two unipolar electrograms (**Figure 10**). Experimental studies have demonstrated that the most accurate algorithm for activation detection of the bipolar electrogram is the so-called Peak Algorithm. This algorithm states that as bipolar electrograms are considered to be the first derivative of unipolar signals, the moment of the maximum amplitude of the bipolar electrogram corresponded with the timing of the maximum negative slope of the intrinsic deflection of a unipolar electrogram[77;78]. However, the peak-algorithm assumes that the shape and velocity of the wavefront remains constant when its propagates through the myocardium, which is most often not the case (e.g. in non-uniform anisotropic tissue).

The amplitude of electrograms is determined by numerous variables including the area of the dipole layer, the distance between the dipole and the recording electrode, intracellular and extracellular resistances, electrode-wall contact, properties of the underlying tissue and tissue volume. [79] The amplitude of bipolar electrograms is additionally influenced by the inter-electrode distance and angle between the activation wavefront and recording electrodes; maximum amplitude is recorded when the activation wavefront moves parallel to the recording electrodes. When it moves perpendicular to them, no signal is recorded. Voltages of unipolar electrograms are larger than voltages of bipolar electrograms; an explanation for this is given in **Figure 10 and 11**. **Figure 10** shows a schematic representation of unipolar electrograms recorded by two electrodes positioned parallel to an activation wavefront propagating with a constant velocity (panel A-C). Bipolar electrograms recorded by each electrode pair with variable inter-electrode distances are shown in the right panel ('true bipolar electrograms'). The amplitude of the bipolar electrogram depends on the time delay between the two unipolar electrograms. **Figure 11** shows a schematic representation of unipolar and bipolar electrograms ('clinical bipolar electrograms') recorded by the tip and ring electrode of a catheter positioned parallel to an activation wavefront propagating with a constant velocity. There is a small time delay between activation recorded by the tip and ring electrode. The amplitude of the unipolar electrogram recorded by the ring electrode is smaller than the amplitude of the unipolar electrogram recorded by the tip electrode as the distance between the electrode and activation wavefront is larger (panel A-C). In both **Figure 10 and 11**, the peak-to-peak amplitude of a bipolar electrogram is smaller than the peak-to-peak amplitude of a unipolar electrogram. Only when the maximum voltage at the distal electrode approaches the same time instant as the minimum voltage at the proximal electrode, the negative

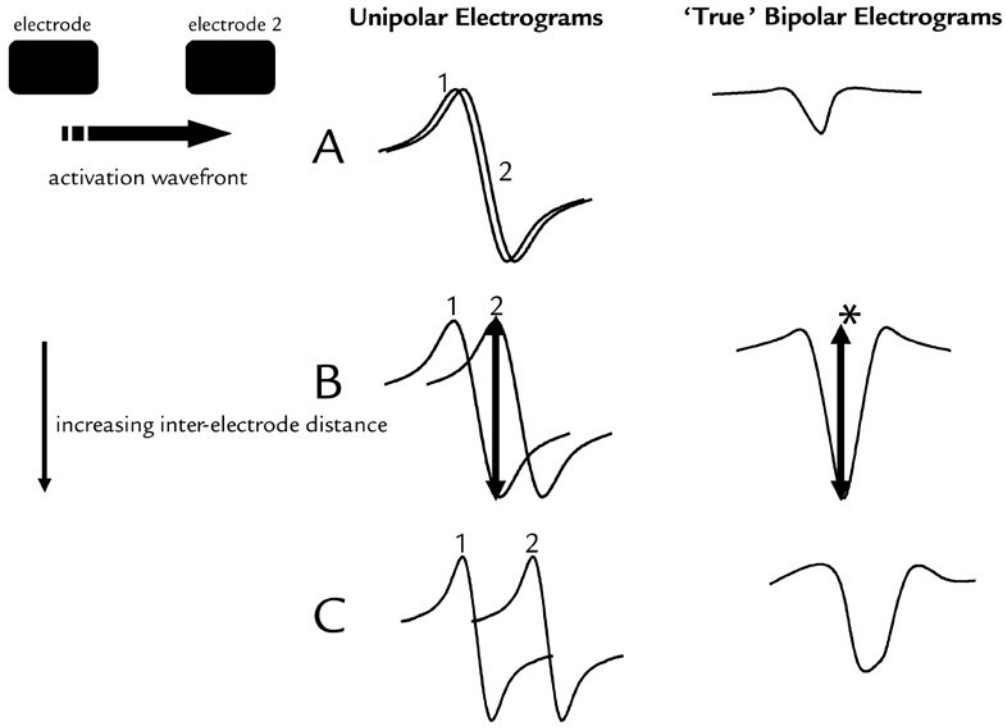

Figure 10.
Unipolar electrograms and corresponding bipolar electrograms recorded by two electrodes with a variable inter-electrode distance positioned parallel to an activation wavefront. The amplitude of the bipolar electrogram is determined by the time delay between the two unipolar electrograms.

deflection of the bipolar electrogram equals the peak-to-peak deflection of the unipolar electrogram (*).

Patterns of activation also influence the morphology of electrograms. For example, single positive deflections arise at borders between excitable and inexcitable tissue or at collisions sites. [79-81]

Particularly the morphology of unipolar electrograms can be distorted by far-field signals as its indifferent electrode is located at a distance from the recording site. In case of a bipolar electrogram, both recording electrodes are positioned close together resulting in less sensitivity for far-field signals and better capability to discriminate local from distant activity. Bipolar electrograms are therefore in clinical practice preferably used.

In addition, the morphology of electrograms is affected by the recording techniques used, such as the diameter of the recording electrode, inter-electrode distances, filter settings and sampling rate of digitization thereby further complicating interpretation of the morphology of extracellular potentials.

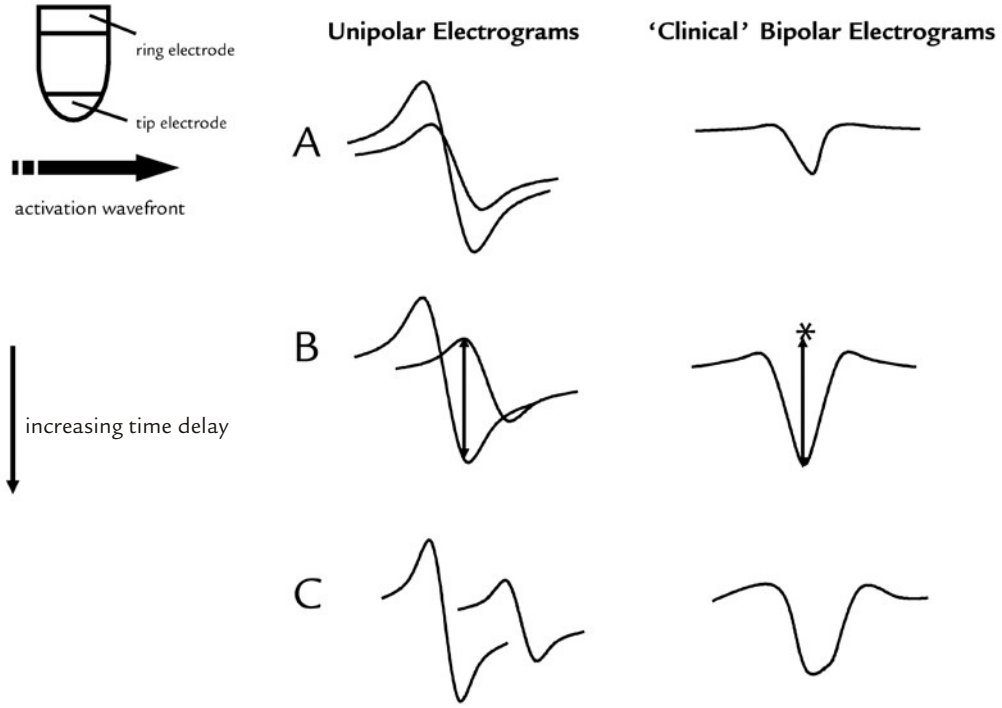

Figure 11.
Unipolar electrograms and the resulting 'clinical bipolar electrograms' recorded by two electrodes with a variable time delay positioned parallel to an activation wavefront. The peak-to-peak amplitude of the bipolar electrograms is lower than the peak-to-peak amplitude of the unipolar electrograms.

Mapping of Regular Atrial Tachyarrhythmias

Mapping of Atrial Flutter

Atrial flutter (AFL) was first reported in 1886 by McWilliams who described regular, rapid excitations of the atrium of an animal. In 1906, Einthoven made electro-cardiographic recordings of AFL and from 1913 mapping studies in animals and humans have been performed in order to elucidate the mechanism underlying AFL.

The surface electrocardiogram of AFL shows a regular tachycardias with absence of an isoelectric baseline between atrial deflections in at least one lead. [82] Based on the rate and response to atrial pacing, Wells et al. subdivided AFL in two different types. [83] The rate of type I AFL ranged from 240 to 340 beats per minute and could be entrained and interrupted by pacing at cycle lengths shorter than the tachycardia cycle length whereas

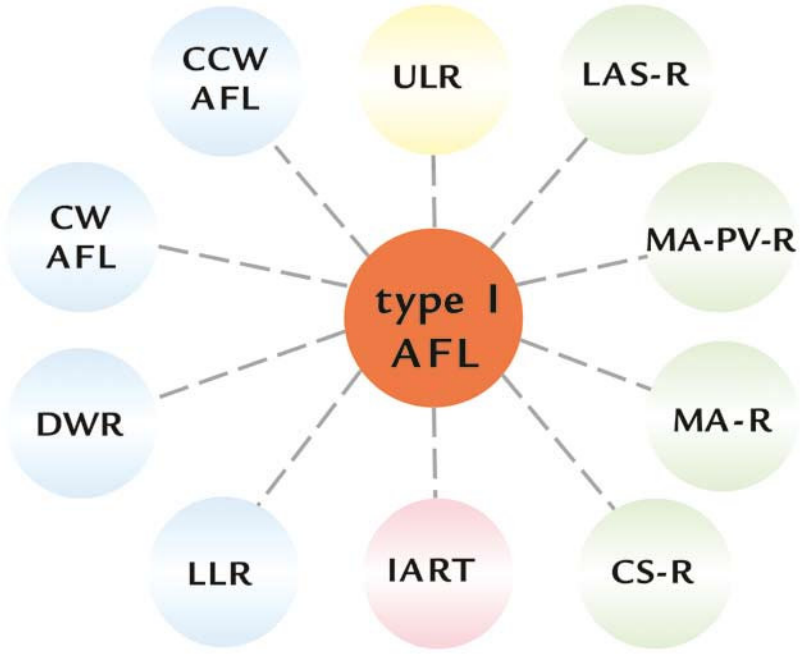

Figure 12.

Classification of different types of AFL. According to cavotricuspid isthmus dependent conduction, AFL is subdivided in typical and atypical AFL.

Blue indicates a right atrial cavotricuspid isthmus dependent macroreentry circuit, yellow a right atrial non-cavotricuspid isthmus dependent macroreentry circuit, green a left atrial macroreentry circuit and red either a right or left atrial macroreentry circuit.

CCW = counterclockwise, CW = clockwise, DWR = double wave reentry, LLR = lower loop reentry, IART = intra-atrial reentry tachycardia, ULR = upper loop reentry, LAS = left atrial septal reentry, MA-R = mitral annulus reentry, MA-PV = mitral annulus – pulmonary vein reentry, CS-R = coronary sinus reentry.

type II AFL was faster (rate ranging from 340 to 433 beats per minute) and could not be influenced by pacing. Numerous mapping studies have been performed in patients with type I AFL and it appeared that type I AFL could be distinguished into different types of AFL, including typical, right atrial cavotricuspid isthmus dependent AFL, atypical right atrial non-cavotricuspid isthmus dependent AFL and left atrial flutters (**Figure 12**). [84-94]

Typical Counterclockwise and Clockwise Atrial Flutter

Typical counterclockwise AFL is the most frequently occurring AFL type (> 90%) and is characterized by inverted P waves in lead II, III, aVF and a biphasic or positive P wave in V1 that transition to negative flutter waves in V6.[87;89;95] The typical P wave consists of a slowly descending segment followed by a rapid negative deflection and a sharp upstroke with a minor overshoot (panel A **Figure 13**).[87] Analysis of flutter wave morphology has

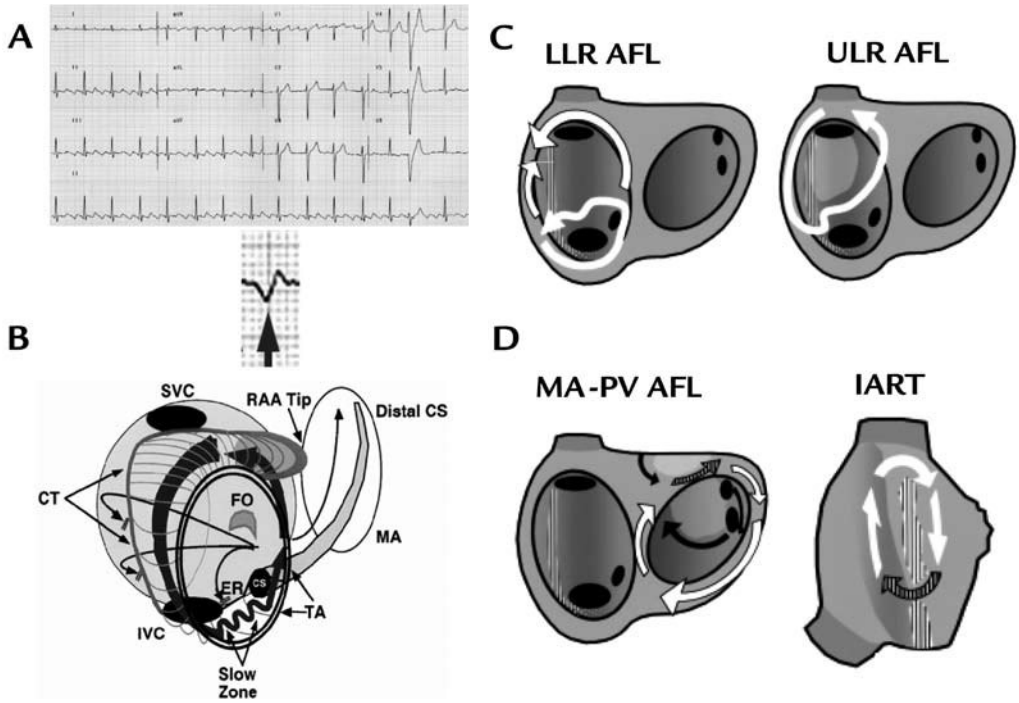

Figure 13.

Panel A: surface electrogram of a typical counterclockwise AFL. Characteristics of flutter waves are a slowly descending segment followed by a rapid negative deflection and a sharp upstroke with a minor overshoot.

Panel B: AFL is caused by a right atrial macro-reentry circuit. During counterclockwise AFL, there is a peritricuspidian counterclockwise rotation of the reentry wavefront which activates the septum and posterior wall in a caudocranial direction and the lateral and anterior wall in a craniocaudaal direction.

Panel C: schematic representations of the reentry circuits of several types of AFL. The white arrows indicates the main activation direction.

CCW = counterclockwise AFL, CW = clockwise AFL, LLR = lower loop reentry, ULR = upper loop reentry, MA-PV-R = mitral valve annulus-pulmonary vein reentry, IART = intra-atrial reentry tachycardia.

demonstrated that a relative large terminal positive component of the flutter wave in the inferior leads is associated with structural heart disease and left atrial dilatation.[96] Mapping studies revealed that AFL is caused by a macro-reentry circuit confined to the right atrium. During counterclockwise AFL, there is a peritricuspidian counterclockwise rotation of the reentry wavefront which activates the septum and posterior wall in a caudocranial direction and the lateral and anterior wall in a craniocaudaal direction (panel B **Figure 13**).[95;97-101] The anterior and posterior boundary of this reentry circuit consists of respectively the tricuspid valve and an area of conduction block between the venae cavae. An isthmus of (slow) conduction is located in the inferior part of the right atrium. The anterior border of the entrance to this isthmus (posterior, lateral or subeustachian isthmus) is formed by the tricuspid annulus and the posterior border by the orifice of the inferior caval vein (the Eustachian ridge) and the terminal crest. The exit of the isthmus is located between the anterior edge of the coronary sinus and the tricuspid annulus (septal or medial isthmus). In patients with a typical clockwise AFL, the reentry pathway is similar as during typical counter-clockwise AFL. The wavelet now conducts in a clockwise direction around the tricuspid valve which gives rise to positive P waves in II, III and aVF, wide biphasic or inverted P waves in V1 and upright P waves in V6. [87;95] Endocardial mapping studies in patients with a 'flutter-like' surface electrocardiogram revealed the existence of two other types of typical right atrial cavotricuspid isthmus dependent reentry circuits including the double wave re-entrant and lower loop re-entrant circuit. Double wave reentry has sofar only been observed as an unstable rhythm which arose when during typical AFL an extrastimulus was delivered between the tricuspid isthmus and Eustachian ridge. [92] This resulted in two simultaneously propagating wavefronts within the same reentry circuit. [94;102] Lower loop reentry occurred when during typical AFL an epicardial breakthrough emerged at the lower lateral right atrial wall generating two separate wavefronts. One wavefront propagated upwards in the atrial septum in a counterclockwise direction where it collides in the high lateral wall with another wavefront originating from the epicardial breakthrough which propagated in a clockwise direction along the lateral free wall. A part of the counterclockwise wavefront propagated through the base of the right atrium, the cavo-tricuspid isthmus, a portion of the smooth right atrium and the lower segment of the terminal crest (lower loop re-entrant circuit: panel C **Figure 13**). Transition from typical AFL to lower loop AFL was associated with shortening of the AFL cycle length. Lower loop reentry was also not a stable rhythm and either alternated with typical AFL (partially isthmus-dependent short circuit flutter) or progressed to AF.[94;102] As perpetuation of typical AFL is depended on conduction through the cavotricuspid isthmus, elimination of typical AFL by catheter ablation is aimed at interrupting the reentry circuit by creating a continuous and transmural lesion at the cavotricuspid isthmus.[103] The reported long-term success rate of typical AFL ablation is high (> 90%) and complications are rare, which makes catheter ablation a safe and efficacious therapeutic option.

Atypical Atrial Flutter

In a minority of the patients presenting with a 'flutter-like' surface electrocardiogram, mapping revealed an atypical AFL. The hallmark of an atypical AFL is the presence of a non-cavotricuspid isthmus dependent reentry circuit which is located in the right and/or left atrium. The use of sophisticated mapping systems allowed identification of different types of atypical AFL, including upper loop reentry, left atrial reentry and incisional reentry (panel C and D figure 13).[88;93;102-106] During upper loop reentry, the re-entrant wavelet propagates in the upper portion – in either a clock or counterclockwise direction of the right atrium – around the superior caval vein and through the terminal crest which serves as a functional obstacle.[89;102] This type of atypical AFL is eliminated by interrupting conduction through the crista terminales gap. In case of atypical left atrial flutter, the re-entrant circuit is bordered by anatomical structures (pulmonary veins, mitral valve), zones of slow conduction or electrically silent regions. [103;104;107] These re-entrant circuit are complex and contain often more than one loop. In patients with mitral valve annular flutter, the activation wavefront propagates in a either clockwise or counterclockwise direction around the mitral annulus.[104;107;108] The posterior boundary of this reentrant circuit is frequently formed by low voltage areas. Mitral valve annular flutter can be terminated by creating a linear lesion from the mitral valve annulus to either scar tissue or one of the pulmonary veins. Marrouche et al. described a reentry circuit propagating around the left septum primum (left atrial septal flutter) which was terminated by creating a linear lesion from the left septum primum to the right inferior pulmonary vein or from the septum primum to the mitral annulus.[109] Another rare type of AFL described is coronary sinus AFL; the reentry wavefront during coronary sinus flutter conducts from the coronary sinus to the lateral left atrial wall, down to the interatrial septum and back to the coronary sinus.[108] Elimination was achieved by creating a circumferential lesion around the coronary sinus os. Double loop reentry has also been observed in the left atrium; one wavefront rotated around one or more pulmonary veins and another wavefront around scar tissue areas in the posterior wall of the left atrium. Though reports on ablation of atypical AFL are still limited, the initial results seem promising.

Intra-Atrial Reentry Tachycardias

Mapping studies of reentrant AT in patients who have had prior cardiac surgery, e.g. for congenital heart defects demonstrated that the macro-reentrant circuits were bordered by prosthetic materials, scar tissue, suture lines or anatomical structures. These so-called intra-atrial reentry tachycardias are difficult to ablate as the reentry circuits often contain multiple (dead-end) pathways embedded within areas of scar tissue.[110] In addition, several circuits can be present within one patient. Compared to typical AFL, the cycle length of an intra-atrial reentry tachycardia is usually longer (270-450 msec).[111] The reported results of ablative therapy of intra-atrial reentry tachycardias is variable (70-100%) which

is probably due to the differences in the complexity of congenital heart defects of the study population. Importantly, the outcome has improved since the introduction of novel 3-dimensional electro-anatomical mapping techniques.

Focal Atrial Tachyarrhythmias

Focal atrial tachycardias (FAT) is defined as an AT originating from a circumscribed region from where it expands centrifugally to the remainder of the atrium.[112] Spread of activation from the focal area does not necessarily has to be radially as conduction can be directed by anatomical or functional barriers.[113] FAT origins are commonly found along the long axis of the terminal crest, the right atrial appendage, the para-Hisian region, the coronary sinus os region, the tricuspid annulus, the left atrial appendage, the mitral annulus ring and the orifices of the pulmonary veins.[114;115]

The surface electrogram of FAT typically consists of discrete p waves separated by an isoeletrical baseline.[112] However, in the presence of conduction disturbances, intra-atrial activation extends over a large proportion of the cycle length thereby giving rise to flutter-like waves.[112] The mechanism underlying FAT can be either micro-reentry (reentry within an area with a diameter of < 2 cm) enhanced automaticity or triggered activity.[112]

FAT based on automaticity are insensitive to verapamil and can only be transiently suppressed with adenosine.[116] Automatic FAT show a warming up (progressive rate increase at tachycardia onset) and cooling down (progressive rate decrease before termination) phenomenon. They are often incessant and can lead to congestive heart failure. Non-automatic FAT (triggered activity or micro-reentry) can be initiated and terminated by programmed electrical stimulation, induced with catecholamine and terminated by adenosine.[117;118] FAT due to an automatic mechanism are mainly found in pediatric patients whereas non-automatic FAT occur more frequently in geriatric patients.[116] Kammeraad et al. described characteristics of 38 patients with non-automatic FAT (defined as FAT inducible by pacing maneuvers).[119] The majority of these patients were women without structural heart disease and the FAT originated mainly from the right atrium (terminal crest, right atrial appendage) though also left atrial foci were found (pulmonary veins and left atrial appendage).

Insight into the mechanism of termination of FAT by adenosine has been provided by Higa et al.[113;120] By using non-contact mapping they showed that termination of FAT by adenosine was preceded by a decrease in voltage reduction at the FAT origin, followed by disappearance of focal activation. The observed voltage reduction was thought to be the result of concentration dependent inhibition of spontaneous discharge.[113]

Regardless the mechanism, FAT can effectively be treated by catheter ablation.[121-125] Ablation is targeted at the area of earliest endocardial activity (activation usually preceding the P wave by 30 to 50 msec).[121;122;126] Electrograms recorded from this region commonly consist of fractionated potentials.[126;127] In case of a unipolar potential, fractionated potentials preceding a negative QS pattern with sharp deflections have been repeatedly observed.[124]

Mapping of Irregular Atrial Tachyarrhythmias

The surface electrocardiogram of atrial fibrillation (AF) is characterized by rapid, low-amplitude oscillations and irregular ventricular rate. However, the surface ECG does not provide any information about the different underlying mechanisms of AF (**Figure 14**).

The first experiment demonstrating that AF can result from different mechanisms was performed by Moe et al.[128] In the isolated canine atria, they compared AF initiated by rapid pacing from the right atrial appendage during either vagal stimulation or application of aconitine. Isolation of the aconitine spot resulted in prompt recovery of sinus rhythm whereas AF continued after isolation of the pacing site during vagal stimulation. This experiment suggested that aconitine-fibrillation is based on an ectopic focus with a high frequency discharge resulting in non-uniform excitation of the atria. This kind of fibrillation was described as "fibrillatory conduction", because perpetuation of AF depended on the persistence of a single focus. On the other hand, acetylcholine-fibrillation continued independently from the site where it was initiated ("true fibrillation"). The features of "true fibrillation" were explained by Moe's multiple wavelet hypothesis.[129] In this hypothesis, it was postulated that persistence of AF depended on the average number of circulating wavelets. If the total number of wavelets increased, the chance of extinguishment and termination of AF would become smaller.

A number of mapping studies of induced, paroxysmal and chronic AF in animal models and in patients contributed to the insight of the possible mechanisms of AF; the results of these studies are summarized in **Table 1 and 2** and discussed below.

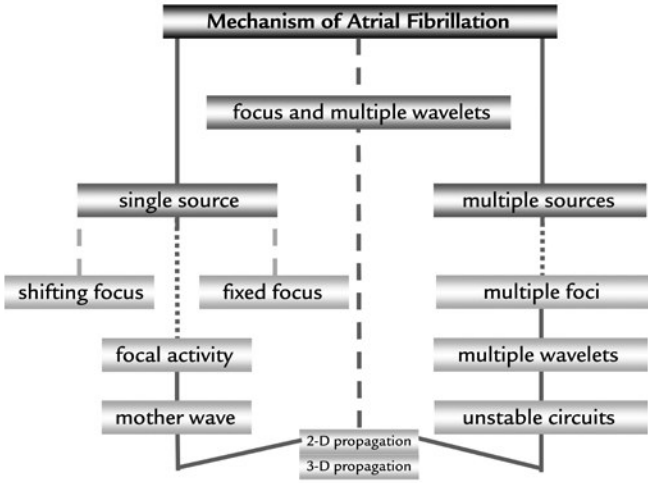

Figure 14.

Possible mechanisms underlying AF. AF can be the result of a single source, multiple sources or co-existence of a focus and multiple wavelets. A single source (focus or mother wavelet giving rise passive daughter wavelets) can be either stationary or wandering. In case of multiple sources, multiple foci, multiple wavelets or numerous unstable reentry circuits excite the atria irregularly. The complexity of conduction during AF is further increased when propagation of fibrillation is 3-dimensional.

Table 1. **Animal models of atrial fibrillation**

year	author	animal model	mechanism	remarks
1914	Garrey	electrically induced AF	focus + fibrillatory conduction	
1948	Scherf	aconitine induced AF	focus + fibrillatory conduction	
1967	Goto	rabbit atria – aconitine induced AF	focus + fibrillatory conduction	
1969	Azuma	rabbit atria – aconitine induced AF	focus + fibrillatory conduction	
1959	Moe	rabbit atria – aconitine induced AF	focus + fibrillatory conduction	
		rabbit atria – electrically induced AF	true fibrillation	
1982	Allessie	isolated canine atria		
		pacing induced AF during Ach infusion	true fibrillation	multiple wavelets
1992	Schuessler	canine – right atrium		figure of eight closed loop
		pacing induced AF during Ach infusion	focus + fibrillatory conduction	reentrant circuit
1997	Kumagai	canine-atria: sterile pericarditis model	focus + fibrillatory conduction	closed loop reentry
		pacing induced AF		
1998	Matsuo	canine-atria: sterile pericarditis model	focus + fibrillatory conduction	single stable reentrant circuits, mainly around pulmonary veins
		pacing induced AF		
1992	Wang	continuous vagal stimulation	focus + fibrillatory conduction	closed loop reentrant circuit
1993	Wang	continuous vagal stimulation	focus + fibrillatory conduction	closed loop reentrant circuit
1998	Skanes	langendorfer perfused sheep heart	focus + fibrillatory conduction	closed loop reentrant circuit
		pacing induced AF during Ach infusion		closed loop reentrant circuit
1998	Wu	isolated canine atria	intra-mural reentry (pectinate muscle)	
		pacing induced AF during Ach infusion		
2000	Berenfeld	langendorfer perfused sheep heart	focus + fibrillatory conduction	
		pacing induced AF during Ach infusion		
2000	Mandapati	langendorfer perfused sheep heart	focus + fibrillatory conduction	closed loop reentrant circuit
		pacing induced AF during Ach infusion		

2001	Derackhchan	canine atria-pacing induced AF during Ach infusion		macro-reentry
2003	Stambler	canine atria-pacing induced heart failure	focus + fibrillatory conduction	delayed after depolarizations?
2003	Okuyama	canine atria-pacing induced congestive heart failure	focus + fibrillatory conduction	
2003	Arora	canine atria-pacing induced AF during Ach infusion	focal activity and reentry	

AF = atrial fibrillation, Ach = acetylcholine

Table 2. Mapping of atrial fibrillation in humans

year	author	Study Population	mechanism	location	remarks
1991	Cox	wpw-syndrome	true fibrillation, focus + fibrillatory conduction	RA+LA	multiple wavelets, large reentrant circuits
1997	Konings	wpw-syndrome		RAFW	leading circle reentry, random reentry, type I, II and III AF
1996	Harada	MVD+CAF	focus + fibrillatory conduction	LA	
1996	Sueda	MVD+CAF	focus + fibrillatory conduction	LA	
1997	Holm	CAF+MVD+AVD		RA	repetitive focal patterns of activation
1998	Haissaguerre		pulmonary vein foci		
2000	Harada	MVD+CAF	focus + fibrillatory conduction	LA	
2000	Pappone		pulmonary vein foci		
2000	Schilling	CAF			type I, II and III AF
2001	Gaita	Lone AF	X		intra-atrial dispersion AFCL, LA: shortest AFCL
2002	Sahadevan	CAF	focus + fibrillatory conduction	RA+LA	
2002	Wu	CAF+MVD+AVD	focus + fibrillatory conduction	RA+LA	
2003	Peters	CAF	multiple wavelets + repetitive activation pattern		
2004	Kanagaratnam	MVD+CAF	focus + fibrillatory conduction		concurrent multiple repetitive focal activation
			reentrant circuit		RA

CAF = chronic AF, MDV = mitral valve disease, AVD = aortic valve disease, RA : right atrium, LA: left atrium, RAFW: right atrial free wall, WPW = Wolff-Parkinson White syndrome, AFCL = AF cycle length.

Electrically Induced AF

The first experimental evaluation of Moe's multiple wavelet hypothesis was performed by Allessie et al.[130] They demonstrated a continuous beat-to-beat change in activation pattern. Figure 15 shows a series of consecutive excitation maps of a canine right atrium during 0.5 second of acutely induced AF. For comparison, the right lower panel shows the activation map during sinus rhythm. As can be seen from these maps, there was a continuous beat-to-beat change in activation pattern. The critical number of wavelets in both right and left atria necessary to perpetuate AF was estimated to be between three and six.

The first mapping study of electrically induced AF in humans was performed by Cox et al. in 1991 in patients with the Wolff-Parkinson White syndrome undergoing cardiac surgery for interruption of their accessory atrio-ventricular pathway.[24] AF was induced by burst-pacing and the right and left atria were mapped using several epicardial templates containing 160 bipolar electrodes, with an inter-electrode distance varying between 5 and 10 mm. In Figure 16, four examples are shown of single isochronal maps as recorded during induced AF. In the upper left panel, a wavefront rotated counterclockwise around a line of conduction block along the sulcus terminalis. The upper right panel shows a large reentry circuit propagating clockwise around a line of conduction block located along the sulcus terminalis and extending to the free wall of the right atrium. In the lower left panel, the impulse propagated clockwise around a small area of conduction block located close to the superior caval vein. The lower right panel reveals a small reentry circuit in the left atrium located between the pulmonary veins and the mitral valve. Results of this first clinical mapping study were consistent with previous experimental studies in the isolated canine heart, revealing reentry at multiple sites as the underlying mechanism of AF. All patients demonstrated non-uniform conduction around regions of bi-directional block resulting in multiple discrete wavefronts. Although anatomical obstacles such as the pulmonary and caval veins were involved in some reentry circuits, reentry also occurred without the involvement of anatomical obstacles. Sometimes, functional conduction block was associated with specific atrial structures such as the terminal crest. In 6 of 13 patients, a reentry circuit could be identified in the right atrium circulating around the sulcus terminalis. In the left atrium, reentry circuits were more difficult to document and seemed to occur more fleetingly. In all patients, multiple wavefronts and lines of conduction block were found both in the right and left atrium.

A limitation of this first mapping study in humans with AF was that only single maps were presented and that beat-to-beat changes in activation during AF were not analysed.

High density mapping of electrically induced AF was performed by Konings et al. in 25 patients with the Wolff-Parkinson White syndrome.[131] During cardiac surgery, the free wall of the right and left atrium were mapped consecutively with a spoon electrode containing 244 unipolar electrodes (diameter 4 cm, spatial resolution 2.25 mm). The activation pattern of the right atrial free wall demonstrated a high intra- and inter-individual

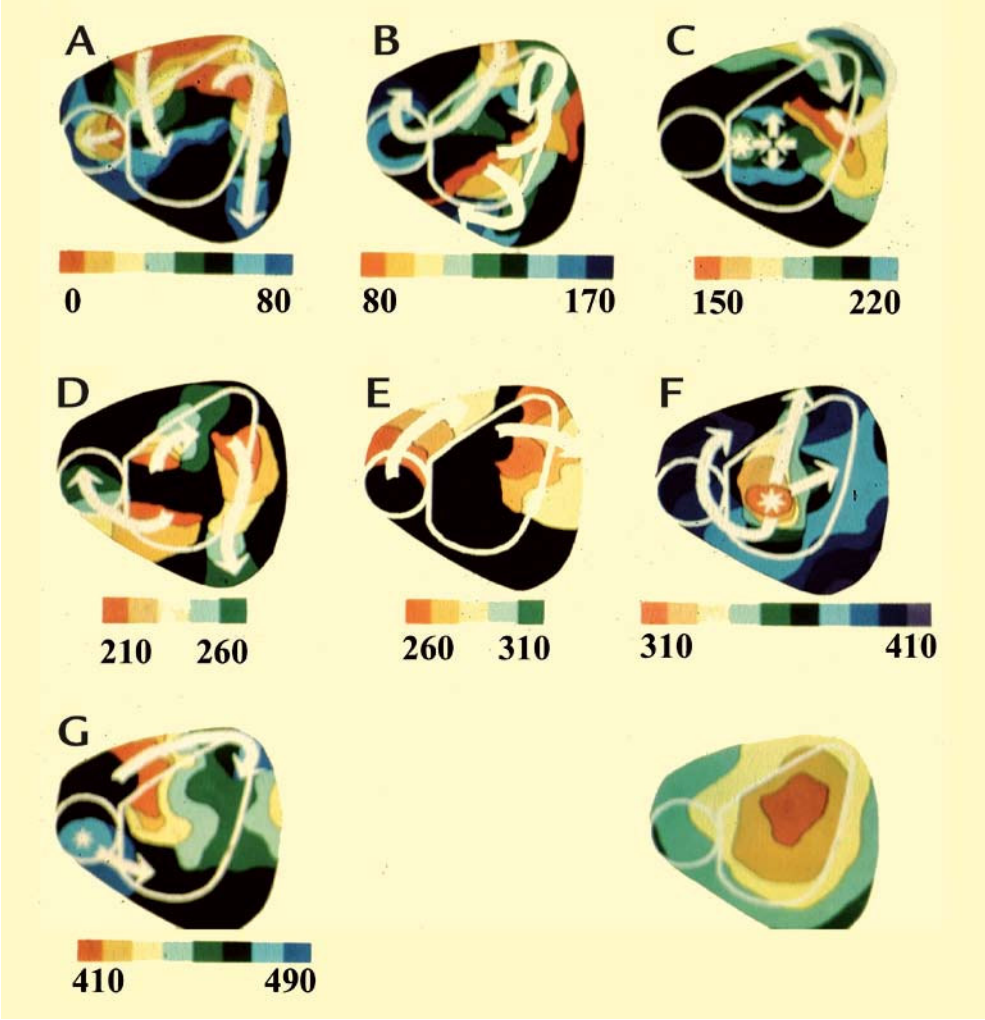

Figure 15.
Endocardial excitation maps of the right atrium during 0.5 second of self-perpetuating AF in the isolated canine heart. The maps were reconstructed from simultaneous recordings of 192 electrograms from a template containing 480 electrodes with an inter-electrode distance of 3 mm. The propagation pattern is visualized by colors, each representing 10 ms. In the lower right panel, an activation map during sinus rhythm map is given. During AF, multiple wavelets can be clearly identified. The asterisks indicate sites of endocardial breakthrough of impulses probably originating from the left atrium (panel C, F and G). (adapted from Allessie et al.).[130]

variability. The activation patterns ranged from well-organized activation consisting of a single planar wavefront to completely disorganized activation by multiple wavefronts propagating in different directions. The degree of organization was related to the median AF cycle length; short median AF cycle lengths were associated with higher degrees of disorganization. Based on the complexity of activation, three different types of AF

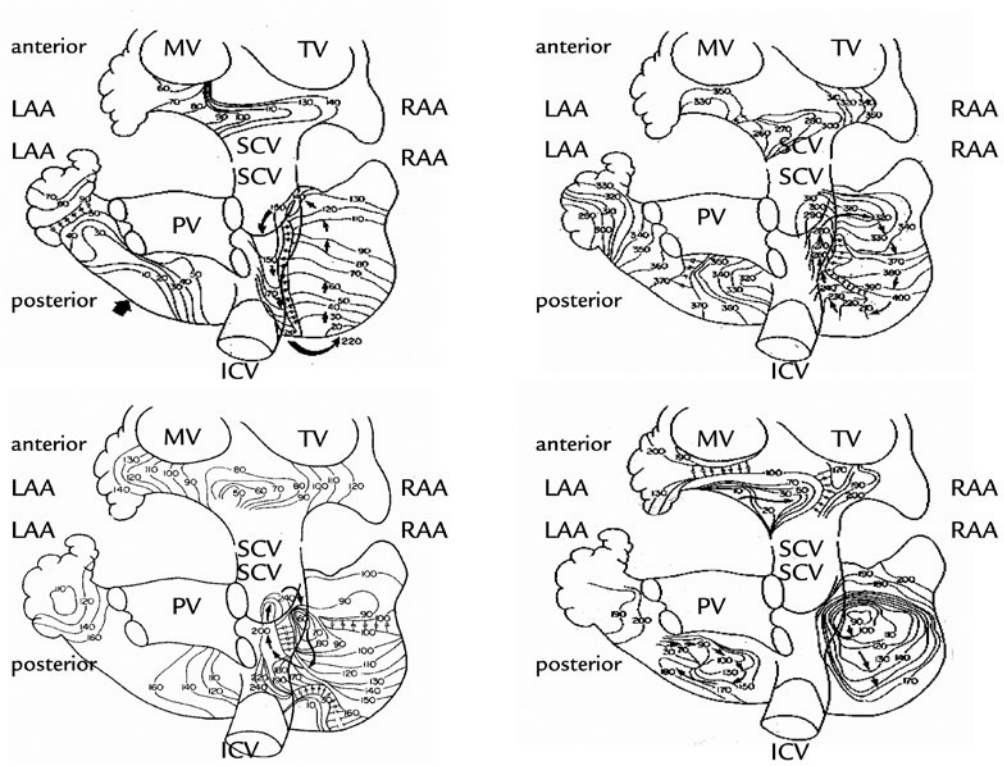

Figure 16.

Four examples of single isochronal maps of the right and left atrium constructed during electrically induced AF in humans. The anterior and posterior surface of the atria are shown together in a 2-D plane.
The maps were constructed using epicardial templates, containing 160 bipolar electrodes with an interelectrode distance ranging between 5 and 10 mm. The small arrows indicate the main direction of the activation waves. The thick arrow in the upper left panel points to retrograde activation from the ventricles at the site of the accessory pathway.
SCV = superior caval vein, ICV = inferior caval vein, PV = pulmonary veins, RAA = right atrial appendage, LAA = left atrial appendage, MV = mitral valve, TV = tricuspid valve. (modified from Cox et al.).[24]

were distinguished. During type I, most of the time single broad wavefronts propagated across the right atrial free wall. Only small areas of slow conduction or conduction block occurred, not disturbing the main course of the large fibrillatory waves. This type of AF probably reflects the presence of macro-reentry with involvement of anatomical obstacles. During type II AF, either one wavefront propagating with marked local conduction delay or two separate wavefronts were present. During type III, multiple fibrillatory waves were recorded simultaneously in the mapping area with a diameter of 4 cm. These multiple wavelets were separated by lines of functional intra-atrial conduction block. The incidence of type I, II and III AF in the small group of 25 WPW-patients was 40, 32 and 28 % respectively. During type III fibrillation, leading circle reentry and random reentry were frequently observed. Incidentally, a focal pattern of activation was recorded on the free wall of the right atrium. These patterns of focal activation were only found as solitary

events and never occurred repetitively. Electrograms recorded at the site of earliest activation were preceded by a small r wave indicating that the focal activation pattern was probably caused by epicardial breakthrough of an activation wave propagating through one of the pectinate muscles.

In Figure 17, isochronal maps of two consecutive beats of each phenomenon are shown together with a selection of unipolar electrograms. In the left panel, an example of leading circle reentry is demonstrated. The activation wave circulated clockwise around a shifting line of functional conduction block. These continuously shifting functional reentry circuits appeared to be unstable and usually disappeared after a few beats. During random reentry, a wavefront re-excites an area that just has been activated by another fibrillatory wave. In the middle panel, one wavefront activated the lower 2/3 of the mapping area

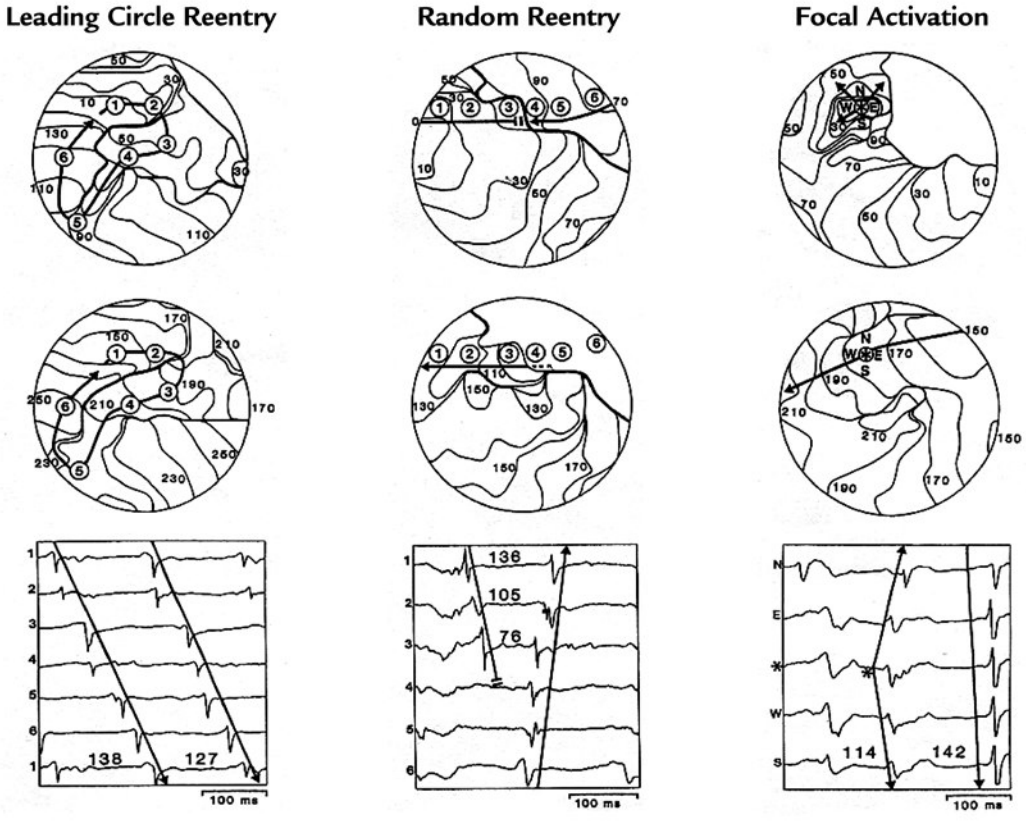

Figure 17.

High density mapping (244 electrodes, diameter mapping area 3.6 cm) of the free wall of the right atrium during electrically induced type III AF in normal human atria. The maps show examples of leading circle reentry, random reentry and a focal activation pattern. Of each of these phenomena, two consecutive isochronal maps are given, together with a small selection of unipolar electrograms. See text for description. (modified from Konings et al.).[131]

from left to the right (t = 0-70 ms). The upper 1/3 of the mapping area was activated by another fibrillatory wave from right to left, entering at t = 70 ms. The first wave activated electrodes 1 to 3 and was blocked between electrodes 3 and 4. The second wave activated electrodes 6 to 4 and was not blocked at electrode 3. Instead, it reentered the relative refractory tail of the first wave and re-excited electrodes 1, 2 and 3 in reverse order (second beat). The electrograms also show the first activation wavefront moving from electrode 1 to 3 and the second wavefront from electrode 6 to 1. Electrode 3 is reentered after only 76 ms showing that in humans the atrial refractory period during AF can be very short. In the right panels an example of focal activation is shown. During the first beat, a new wavefront arises in the upper part of the mapping area (*). From here it spread radially into all directions. This focal activation pattern disappeared again during the second beat and the entire mapping area was now activated by a wavefront entering from the right and propagating to the left.

Breakthrough patterns were also found during optical mapping studies of the right atrial free wall in the isolated sheep heart during electrically induced AF. [42] Breakthrough sites appeared to be confined to the area of the pectinate muscle bundles. Schuessler et al. performed simultaneous endocardial and epicardial mapping of isolated canine atria during sinus rhythm, continuous pacing, premature stimulation and induced tachyarrhythmias. [132] In general, only small differences between endocardial and epicardial activation time (< 1 ms) were found, suggesting that endocardial and epicardial activation occurred more or less simultaneously. Larger differences in endo- and epicardial activation times can be associated with the underlying atrial architecture (pectinate muscles and sites with transmural differences in fiber orientation). During reentry tachycardia, a focal activation pattern was found both on the endocardial and epicardial surface. The sites of earliest activation were spatially disconcordant with a separation of 15 mm between the earliest endocardial and epicardial breakthrough. Simultaneous mapping of the epicardial and endocardial layer during electrically induced acetylcholine-AF in canine atria in congestive heart failure also demonstrated macro-reentrys circuits involving the endocardium and epicardium. [133] In isolated canine atria, pectinate muscles play a role in formation of intra-atrial reentry circuits by either being a part of the reentry circuit or by functioning as a natural anchor of the reentry circuit. These studies thus provide clear evidence of transmural activation during atrial arrhythmias, suggesting the presence of 3-D reentry in some cases.

Spectral analysis of optical recordings was used to determine the presence of dominant circuits during electrically induced acetylcholine-AF.[134] It was found that the activation pattern of the left atrium in general was more regular than that of the right atrium. In some cases, sources of periodic activity, were found appearing as stationary rotors or as sites of epicardial breakthrough. **Figure 18** shows 3 consecutive isochronal maps of the left atrium of a sheep as reconstructed from optical recordings of AF. The site of breakthrough was similar in each map. The lower panels show fast fourier transforms of the

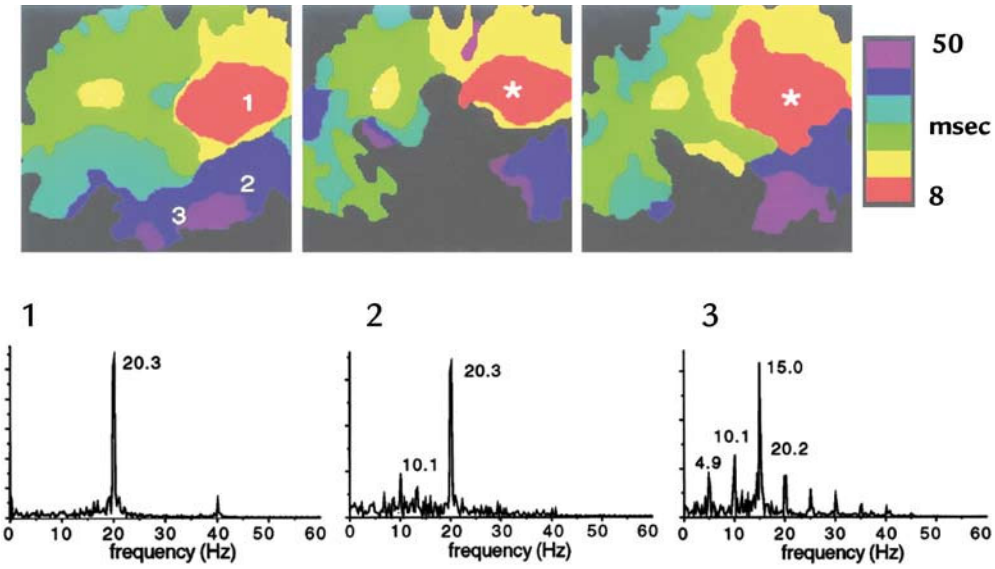

Figure 18.

Upper panel: three sequential isochronal maps of the left atrium from an isolated sheep heart constructed from optical recordings demonstrating a repetitive focal spread of activation. *Lower panel:* fourier transforms of the transmembrane potentials at sites 1, 2 and 3. At all sites, temporal periodicity is demonstrated by the presence of a dominant peak between 15 and 20 Hz. Remote from the dominant source, the activation pattern became more complex reflected by the appearance of additional frequency peaks at sites 2 and 3.[134]

transmembrane potentials at sites 1, 2 and 3. At the site of breakthrough (1), a single dominant peak of 20.3 Hz. was found. Moving away from this dominant source of rapid impulses, the activation became more irregular and multiple peaks now appeared in the spectral analysis. The highest dominant frequency was often found at the left posterior atrial wall where optical mapping revealed the presence of a small stationary vortex (micro-reentry).[135;136] The narrow banded frequency spectra observed in these studies indicate that AF is not a random phenomena and that some degree of organization may be present. Several studies performed in humans have also provided evidence for non-randomness of AF by demonstrating that 'fibrillatory wavefronts have a tendency to follow paths of previous excitation' (linking).[137;138] A higher frequency of dominant sources was associated with a higher degree of fibrillatory conduction. Wavebreaks occurred frequently at the left atrial appendage and right atrial free wall.[139] The wavelets had a short lifespan (< one rotation) suggesting that multiple wavelets during AF are generated by breaking up of high frequency waves when they propagate through heterogeneous tissue. From these studies the authors concluded that Moe's multiple wavelet hypothesis did not offer a robust mechanism of maintenance of AF. However, it should be noted that the frequency of AF in these studies was much higher (20 Hz; 1200/min) then the frequency of atrial fibrillation in humans which ranges between 300 and 420 beats per minute.

Paroxysmal Atrial Fibrillation

Epicardial and endocardial mapping during electrically induced AF in dogs with sterile pericarditis showed that unstable reentry circuits with short cycle lengths were critical for the maintenance of AF. [57] **Figure 19** shows an example of the activation of the right and left atrium during 1.2 seconds of AF. The first two maps show a reentry circuit located at the right atrial free wall (orange) which disappeared in the third map. A similar circuit reappeared in maps 7-11. Another reentry circuit (green) was found in the left atrium circulating around the pulmonary veins. In most maps a reentry circuit comprising the

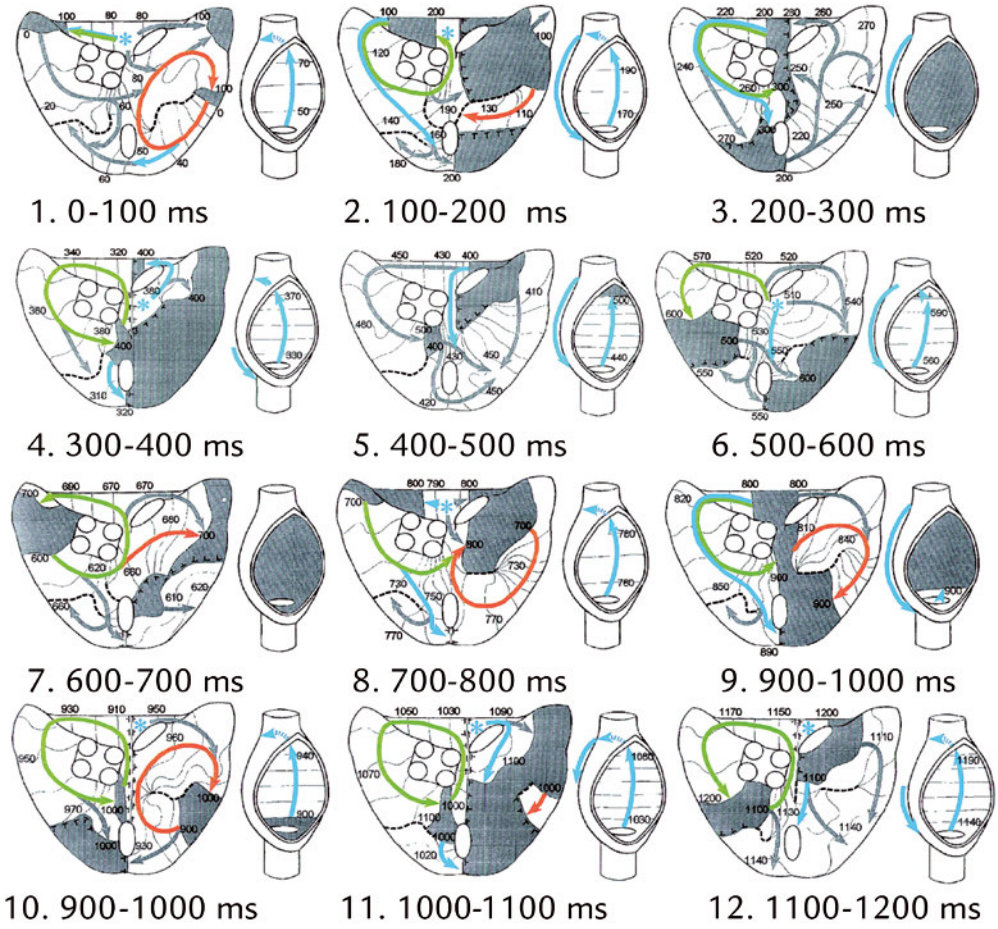

Figure 19.

Twelve consecutive isochronal maps of both atria during 1.2 seconds of electrically induced AF in a dog with sterile pericarditis. Each map covers a time window of 100 ms. The maps were reconstructed using epicardial templates containing 186 bipolar electrode pairs and endocardial multipolar catheters (12-, 20 or 24 poles with an interelectrode distance of 1 or 2 mm). The isochrones are drawn at 10 msec intervals. The colored arrows indicate different unstable reentry circuits. Dashed lines represent lines of functional block. Asterisks indicate sites of epicardial breakthrough. Regions which are not activated in the time window of 100 ms are gray. (modified from Kumagai et al.). [57]

interatrial septum and Bachmann's bundle was present. Based on the hypothesis that this circuit was critical for the maintenance of AF, the conduction through Bachmann's bundle was blocked by ablation. After the ablation of Bachmann's bundle, AF was no longer inducible. [55]

Mapping studies in patients with paroxysmal AF showed that AF could be initiated by a rapidly firing focus. The majority of these ectopic atrial premature beats originated from one of the pulmonary veins. Sometimes ectopic beats originating from the superior caval vein, terminal crest, coronary sinus, or left atrial posterior free wall initiated a paroxysm of AF. Catheter ablation of the focus resulted in a marked reduction of the number of episodes of AF.

Recently, the atrial myocardium within the ligament of Marshall has been suggested as another possible site of focal activity. [140] Epicardial mapping (480 bipolar electrodes) of electrically induced AF in dogs located an area with the shortest AF cycle lengths in the ligament of Marshall or one of the left pulmonary veins. In two dogs, spontaneous episodes of AF were recorded. These episodes started with ectopic beats originating from the ligament of Marshall or high right atrium. During the first seconds of AF, atrial activation was still organized but thereafter it converted to AF. The earliest activation during atrial tachycardia and conversion to AF was recorded from the ligament of Marshall.

Chronic Atrial Fibrillation

Sofar, only a limited number of mapping studies of chronic AF have been performed in patients, mostly during cardiac surgery for mitral valve disease.[141-145] Holm et al. analyzed the activation patterns of the right atrial appendage and posterior wall in 16 patients. [144] Using a mapping array of 56 bipolar electrodes, the occurrence of type I, II and III AF was determined. At the posterior free wall, types I, II and III were present in 27, 40 and 33 % of the patients. In the right atrial appendage, the incidence was 46, 27, and 27 %. The major new finding of this study was that during chronic AF in humans, focal activation of the right atrium occurred repetitively. The right atrial appendage was consistently the origin of this focal activation pattern. An example is given in **Figure 20**. The left part gives a schematic representation of the activation of the right atrial appendage during 51 consecutive beats. In the right part of the Figure, the color maps of beats 33-43 are shown. During beat 33, two wavefronts entered the mapping area from different directions. In the next beat, the mapping area was again invaded by 2 wavefronts but now a third impulse arose from the center of the mapping area (*). During the next beats, a focal activation pattern arose from this site and repeated itself until beat # 43. During beat 44, the mapping area again was again activated by two wavefronts entering from different directions.

Repetitive focal patterns of activation during chronic AF in patients with mitral valve disease were also described by Nitta et al. [145] In their study, epicardial mapping of the atria was performed with an epicardial plaque (253 unipolar electrodes, inter-electrode distance 5-7 mm) covering the right atrial free wall, left atrial free wall and the area between

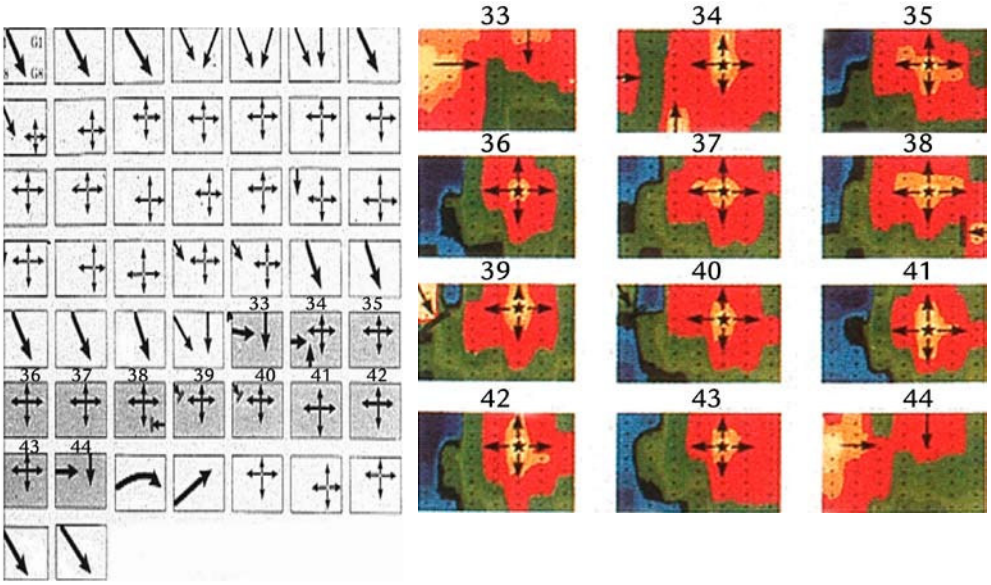

Figure 20.

Repetitive focal activation of the right atrial appendage in a patient with chronic AF.
In the left part, 51 consecutive activation maps are given diagrammatically. The right part shows a series of color maps elucidating a constant site of epicardial breakthrough. The activation maps were reconstructed with an epicardial template of 4 cm containing 56 bipolar electrodes with an interelectrode distance of 3 mm. The asterisks indicate the site of earliest activation. (modified from Holm et al.) [144]

the pulmonary veins. Mapping revealed multiple focal patterns of activation in the both right and left atrium giving rise to fibrillatory conduction (**Figure 21**).
Several mapping studies compared patterns of activation between the right and left atrium. Surprisingly, the activation pattern of the left atrium seemed to be more organized.[142;146] However, in most of these studies the mapping resolution was rather low (only 30 unipolar or 24 bipolar electrodes) and conduction abnormalities occurring in small areas with disorganized conduction might therefore have been easily missed.

Comparison of Paroxysmal and Chronic Atrial Fibrillation

Three experimental studies evaluated differences in the degree of organization between acute and chronic AF. The first study compared acute and chronic AF (142±55 days) in the goat. During acute AF the free wall of the right atrium was activated mainly by broad planar wavefronts (type I AF). In contrast, during chronic AF activation of the right atrium was characterized by type III AF. During chronic AF, the median fibrillation interval was shorter and the incidence of fragmented electrograms was higher. Another mapping study compared right and left atrial activation during acute and chronic AF in dogs, using several epicardial templates with a total of 240 unipolar electrodes. [147]
The atrial rate was higher and activation was more disorganized during chronic AF than

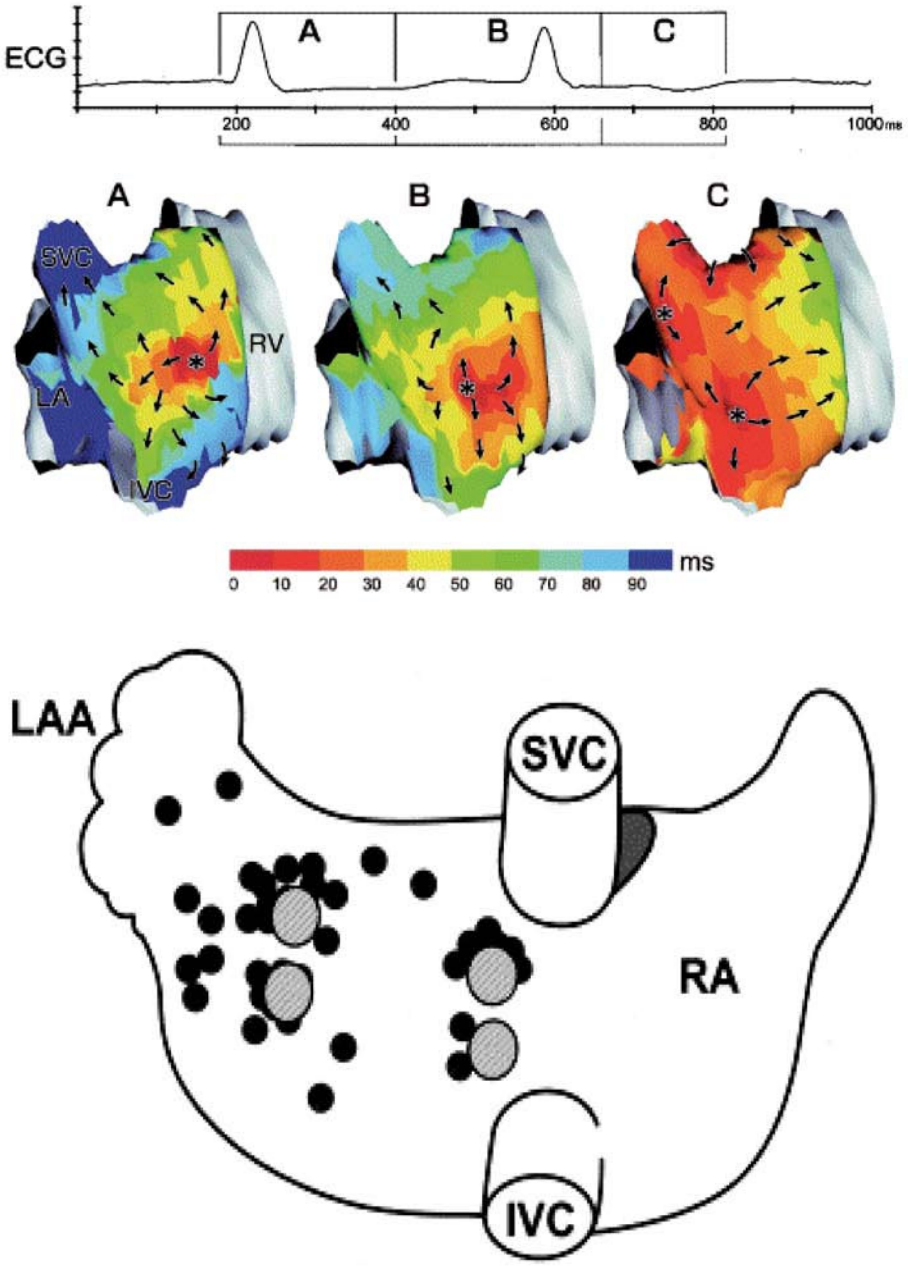

Figure 21.

Upper panel: right atrial patterns of activation maps observed in a patient with permanent AF associated with aortic valve regurgitation and mitral valve stenosis. The cycle lengths of the focal activation are respectively 222, 253, and 162 milliseconds. The site of the earliest activation is indicated as an asterisk (*). *Left panel:* schematic representation of the atria demonstrating the distribution of focal activation in the left atrium. The grey circles indicate pulmonary vein orifices and the black circles electrode locations where focal activation was observed. (modified from Nitta et al.) [145]

during acute AF. During acute AF, in the left atrium the cycle length was slightly shorter than in the right atrium. During chronic AF this difference was enhanced. The activation pattern of the right atrium was similar during acute and chronic AF. On the other hand, in the left atrium during acute AF frequently linking of successive fibrillatory waves was seen, whereas during chronic AF the left atrium was activated by more complex activation patterns.

Akar et al. correlated variation in atrial fibrillation cycle length in dogs with acute AF (rapid atrial pacing) and persistent AF (rapid atrial pacing in dogs with mitral regurgitation) with alterations in atrial structure in order to study the differential effects of electrical and structural remodeling. [148] Comparing acute AF and persistent AF, variation in atrial fibrillation cycle length was larger in the latter group. Morphological changes (myolysis, intercalated disk disruption, mitochondrial swelling) were mild in the acute AF dogs and severe in the persistent AF dogs. Inverse electrical remodeling was observed in dogs with persistent AF after cardioversion to sinus rhythm. After recovery of refractoriness, AF was again induced. Dispersion in atrial fibrillation cycle length was now reduced compared to persistent AF. However, it was still larger than in the acute AF dogs. The findings of this study suggest that the observed dispersion in atrial fibrillation cycle length is caused by abnormalities in atrial structure.

Atrial Fibrillation and Fractionation of Electrograms

Several studies have analysed the relation between fractionation of atrial electrograms and the presence of atrial fibrillation. In these studies, the range of intervals during atrial pacing (S1-S2) resulting in fractionation of atrial electrograms was determined (zone of fractionated activity) in patients with a sick sinus syndrome and/or paroxysmal atrial fibrillation. The zone of fractionated activity was wider in patients with the sick sinus syndrome or paroxysmal atrial fibrillation compared to patients without atrial arrhythmias. The widest zone of fractionated activity was found in patients with both a sick sinus syndrome and paroxysmal atrial fibrillation.[149;150]

The spatial distribution of 'abnormal' bipolar electrograms has also been studied.[151;152] At 12 different sites in the atria, the incidence of abnormal electrograms, defined as electrograms with a duration of ≥ 100 msec and/or ≥ 8 deflections was determined. In patients with the sick sinus syndrome, fractionated electrograms were confined to small regions whereas abnormal electrograms were more widely distributed in patients with paroxysmal atrial fibrillation.[151] The distribution of fractionated electrograms in patients with both AF and the sick sinus syndrome was even more diffuse.[152]

In Wolff-Parkinson-White Syndrome patients, the duration of bipolar electrograms was measured during sinus rhythm at 12 different sites in the right atrium and compared between patients with and without episodes of AF. In patients without AF, only 10% of the electrograms were abnormal whereas in patients with AF, 83% of the electrograms were prolonged and fractionated.[131]

Nakao et al. related fractionation of atrial electrograms with conversion of paroxysmal to chronic AF.[153] Endocardial mapping of the right atrium during sinus rhythm was performed in 69 patients with paroxysmal AF. After a follow-up period of 97±21 months, transition from paroxysmal AF to chronic AF was observed in 17 patients. Chronic AF developed in patients with a relative high incidence of abnormal electrograms at the middle part of the right atrium.[153]

In summary, these studies indicate that local conduction abnormalities, either functional or structural, may play a role in in the pathogenesis of AF. From these data, it could be hypothesized that the magnitude of fractionation may be a suitable parameter to assess the propensity to AF.

Sites with Fractionated Electrograms as Targets for Ablation of Atrial Fibrillation

Bipolar atrial electrograms recorded in patients during AF occurring after cardiac surgery were classified by Wells et al (upper panel **Figure 22**).[154] Type I electrograms were discrete electrograms separated by an isoelectrical baseline free of perturbations. Type II electrograms showed small perturbations around the isoelectrical baseline between discrete atrial signals. No discrete electrograms could be distinguished in type III electrograms. Type IV electrograms were a mixture of type I, II and III electrograms.

The anatomic distribution of different types of electrograms and its relation to the refractory period during electrically induced AF was examined in two dog models (sterile pericarditis versus rapid atrial pacing during 6 weeks).[155] Bipolar fibrillation electrograms were categorized according to the classification of Wells et al.[154] In both groups, disorganized atrial electrograms were found at sites with the longest effective refractory period (right postero-lateral atrium) whereas organized atrial electrograms were found at sites with the shortest effective refractory period (left atrial sites, right atrial appendage). In the goat model of persistent AF, prolongation of atrial fibrillation cycle length by infusion of a class I drug was associated with a significant reduction in the incidence of fractionation.[156] Class I drugs prolong atrial fibrillation cycle length more than atrial refractoriness, thereby widening the excitable gap. Based on these findings, it was hypothesized that the decrease of fractionation was due to widening of the excitable gap as in the presence of a wider excitable gap the wavefront will propagate through muscle which is in a higher state of excitability.

The complexity of endocardial atrial activity during electrically induced AF in humans was analysed by Jais et al. using a multipolar catheter (14 bipolar electrodes, 3 mm interelectrode distance).[157] The study population consisted of 25 patients with paroxysmal AF. The "complex electrical activity time" was defined as the ratio of the total duration of electrograms with fibrillation intervals smaller than 100 ms and the total recording time. Atrial activity was more complex in the left than in the right atrium. In the right atrium the disorganized left atrial activity changed abruptly into more organized activity at the

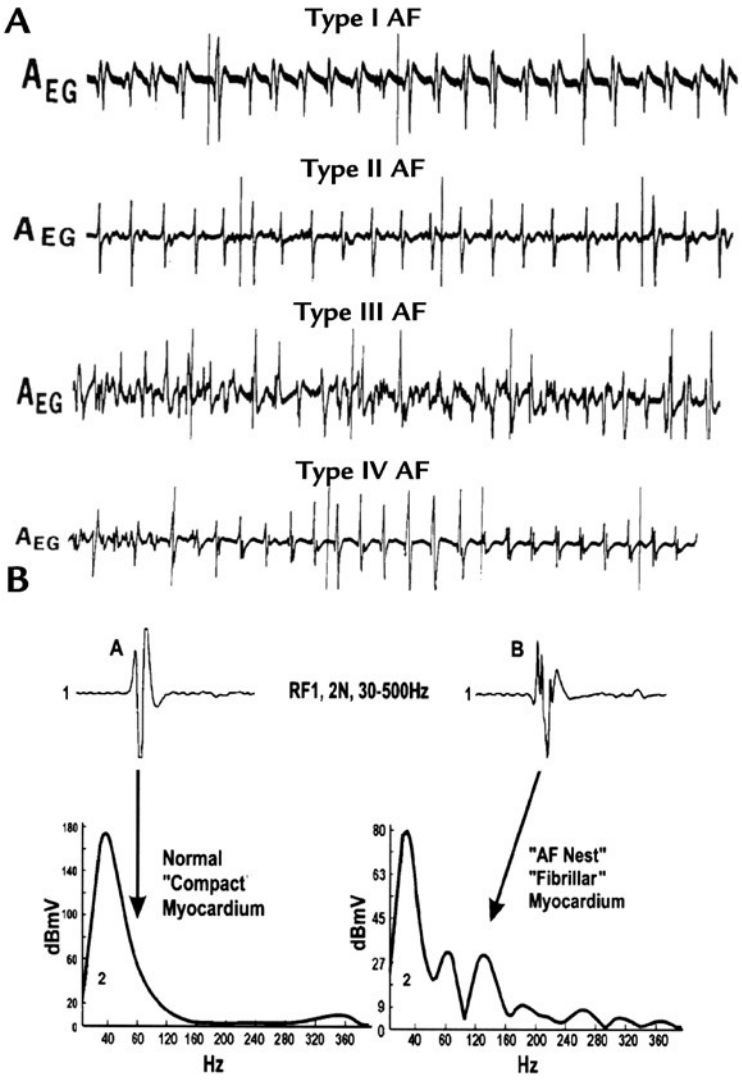

Figure 22.
Panel A: Classification of bipolar electrograms recorded in patients during AF occurring after cardiac surgery by Wells et al.[154] *Panel B:* there is a significant difference in the FFT-spectral analysis of left atrial endocardial potentials representing "compact" and "fibrillar" myocardium. (modified from Pachon et al.)[161]

terminal crest. In the left atrium, atrial activity in the septum and the area between the pulmonary veins was more disorganized than in the appendage and anterior left atrium. Thus, organized fibrillation appeared to be confined to the trabeculated parts of the right and left atrium.

The relation between the morphologies of unipolar fibrillation electrograms and the spatial activation pattern during AF was first studied by Konings et al.[158] Fibrillation electro-

grams were classified as singles, short doubles, long doubles and fragmented potentials. It was found that long double potentials occurred along long lines of functional conduction block whereas fragmented potentials were recorded either during pivoting of fibrillatory waves at the end of a line of block or at areas of slow conduction. Short double potentials were recorded when fibrillatory waves collided. In normal human right atria, no preferential sites for double potentials or fragmented electrograms were found.

Kuck et al. used an electro-anatomical mapping system (CARTO) to analyse bipolar fibrillation electrograms in patients with paroxysmal AF. [159] Fibrillation electrograms were recorded during 45 seconds at 36±12 sites in the left atrium. Electrograms were classified as either type A (regular activation separated by a clear isoelectrical baseline), type B (irregular activation with perturbations of baseline and/or highly fragmented electrograms) or type C (alternation between type A and type B). Type B and C electrograms were equally present throughout the left atrium whereas the incidence of type A electrograms was higher in the upper left pulmonary vein.

Recently, Nademanee et al. proposed mapping of the electrophysiologic substrate as a new approach for ablation of AF.[160] In this study, they presented 121 patients with persistent (n = 26), permanent (n = 38) and paroxysmal (n = 57) AF. Cardiac disease was present in 97 patients (coronary artery disease: n = 47, cardiomyopathy: n = 17, valvular heart disease: n = 14, congenital heart disease: n = 6). Mapping and ablation was performed with the CARTO™ system. Complex fractionated bipolar electrograms were defined as fractionated electrograms containing 2 or more deflections, perturbation of the baseline with continuous deflections, or atrial electrograms with very short cycle lengths (AFCL≤120 ms). Endpoints for ablation were complete elimination of the areas of complex fractionated electrograms, conversion to sinus rhythm (chronic AF and paroxysmal AF patients) and non-inducibility in case of paroxysmal AF.

Areas of complex fractionated electrograms were confined to one, two and three or more specific regions in respectively 23, 43 and 55 patients. Most common sites for complex fractionated electrograms included the inter-atrial septum, pulmonary veins, roof of the left atrium and the coronary sinus. AF terminated in 95% of the ablations. Complex fractionated electrograms were never observed at the right atrium. After one year follow-up, 110 (91%) patients were free of arrhythmia. Based on the results of this study, it was suggested that fractionated electrograms are indicative for atrial regions perpetuating AF.

Pachon et al. also applied an electrogram-guided selective ablation approach in patients with paroxysmal AF. [161] By using fast fourier transforms, recordings were classified as compact or fibrillar myocardium. Compact myocardium represented homogenous fast conduction, whereas fibrillar myocardium ("AF nests") represented heterogeneous conduction (lower panel **Figure 22**). Spectral analysis of compact and fibrillar myocardium consisted of respectively one dominant frequency and multiple dominant frequencies. AF nests were identified during sinus rhythm or atrial pacing, not during AF. Ablation was applied at 41±12 AF nests located around the pulmonary veins, the left atrial roof, left atrial

posterior wall and the interatrial septum. Patients with a higher incidence of AF nests had also more frequent episodes of AF. After ablation, AF was absent in 91%. Hence, these two studies suggest that an electrogram-guided selective ablation approach could be an alternative treatment of AF.

Future Directions

Theoretically, an electrogram-guided selective ablation approach would be advantageous as it results in less tissue destruction. In order to perform such an ablation approach, correct interpretation of a fractionated electrogram is essential.

If a fractionated fibrillation electrogram is recorded, it can be either anatomical or functional in nature. It may be due to physiological properties of the atrial myocardium or to pathologically altered myocardium. Knowledge of the relationship between fractionation and perpetuation of AF is essential for developing an electrogram-guided selective ablation approach. Sofar, it is even unknown whether the incidence and degree of fractionation is associated with stability of AF as differences in fractionation between patients with different types of AF (paroxysmal, permanent or persistent AF) have never been analyzed. In addition, it has never been studied whether fractionation of fibrillation electrograms represent abnormalities in conduction during persistent AF. If future mapping studies demonstrate a relationship between fractionation, atrial architecture (interstitial fibrosis) and abnormalities in conduction, an electrogram-guided selective ablation approach can be further developed.

Post-Operative Atrial Tachyarrhythmias

Atrial Tachyarrhythmias in Patients with Congenital Heart Defects

The incidence of AT in patients with congenital heart defects (CHD) after palliative or corrective cardiac surgery is higher compared to subjects with normal atrial anatomy without prior cardiac surgery.[111;155;162-165] In general, the occurrence of late post-operative AT is associated with a number of variables, including the complexity of congenital heart defects, the number of surgical procedures performed, hemodynamic status and time after cardiac surgery.[111;166-170] AT in this patient group are most often type I typical AFL, intra-atrial reentry tachycardias or AF; focal atrial tachycardias have been less frequently observed.[171-173]

Precipitating factors for development of AT in the setting of CHD are the presence of prosthetic materials and electro-pathological alterations of the atrial architecture. The myocardium is affected by pressure/volume overload and progressive scarring along suture lines or atriotomies.[174] These structural changes give rise to intra-atrial conduction delay and regional differences in dispersion of atrial refractoriness.[175-177] Local conduction abnormalities combined with a higher incidence of premature atrial beats due to stretch of myocardial fibers make these patients more prone to AT.[176-178]

AT in CHD patients may give rise to haemodynamic deterioration, tromboembolic events and even sudden cardiac death. Hence, the quality of life is often severely affected by recurrent symptoms such as fatigue, palpitations and syncope. The morbidity and mortality associated with AT in this patient group justifies an aggressive treatment. [175;177;179-183]

Treatment modalities for AT include anti-arrhythmic drugs, an atrial defibrillator, anti-tachycardia pacing or catheter ablation.[184] Anti-arrhythmic drugs and anti-tachycardia pacing are often not effective.[185;186] Moreover, antiarrhythmic drugs are proarrhythmic, negative inotropic and may aggravate sinus node dysfunction.[186] Antitachycardia pacing can accelerate the tachycardia and increases the risk of conversion to atrial fibrillation.

Considering the low success rate of both pharmacologic therapy and implantable devices combined with the recent developments of endocardial mapping technologies, catheter ablation is an attractive curative treatment option for post-operative AT.[110;185;187-196] Mapping of AT and subsequent ablation is particularly challenging in patients with previous cardiac surgery for transposition of the great arteries, tricuspid atresia, atrial septal defect and tetralogy of Fallot.

Transposition of the great arteries

The common anatomical feature of patients with transposition of the great arteries (TGA) is ventriculoarterial discordance (the aorta is connected to the morphological right ventricle and the pulmonary artery to the morphological left ventricle; upper panel **Figure 23**). TGA is associated with either atrioventricular concordance (complete transposition, D-TGA) or with atrioventricular disconcordance (congenitally corrected TGA, L-TGA).

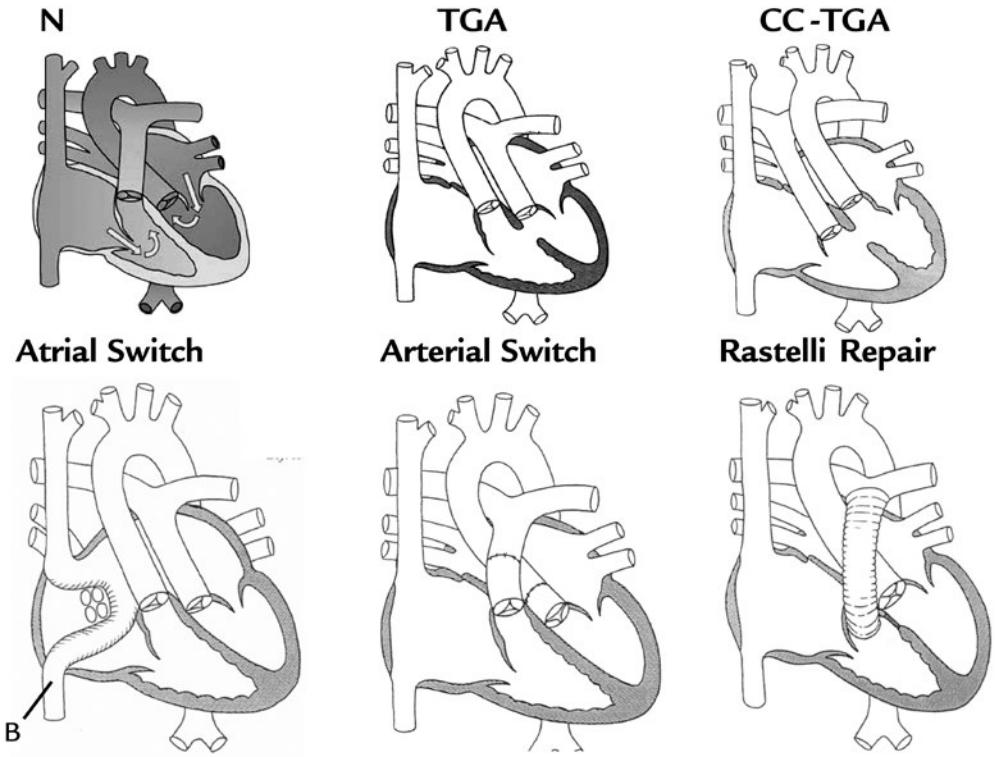

Figure 23.
Upper panel: N: normal relation between the right and left ventricle and great arteries, TGA : the aorta is connected to the morphological right ventricle and the pulmonary artery to the morphological left ventricle, CC-TGA: TGA combined with AV disconcordance.
Lower panel: the Mustard procedure (Venous Switch) is aimed at redirecting systemic venous blood into the morphological right ventricle by using an interatrial baffle (B).
During an arterial switch procedure, the aorta and pulmonary trunk were transected and anastomosed on the contralateral trunk. The Rastelli repair consists of closure of the ventricular septal defect with a patch and placement of a conduit which is connected to the right ventricle and the pulmonary artery.
TGA: transposition of the great arteries, CC-TGA: congenitally corrected transposition of the great arteries.

One-third of the TGA patients also have other cardiac defects, most often a ventricular septal defect or pulmonary artery stenosis.
Cardiac surgery for TGA results in extensive damage of the atria thereby increasing the probability for AT to develop.[175-177;188;197] The first palliative surgical methods developed for TGA were atrial switch procedures, either a Mustard or Senning repair. [183] The Mustard procedure (Venous Switch) is aimed at redirecting systemic venous blood into the morphological right ventricle by using an interatrial baffle (lower panel **Figure 23**). Similar to the Mustard repair, the Senning repair is also aimed at redirecting blood flow now using the atrial septum and wall instead of a baffle. Later, the atrial switch procedure was replaced by an arterial switch procedure (lower panel **Figure 23**). The major advantage

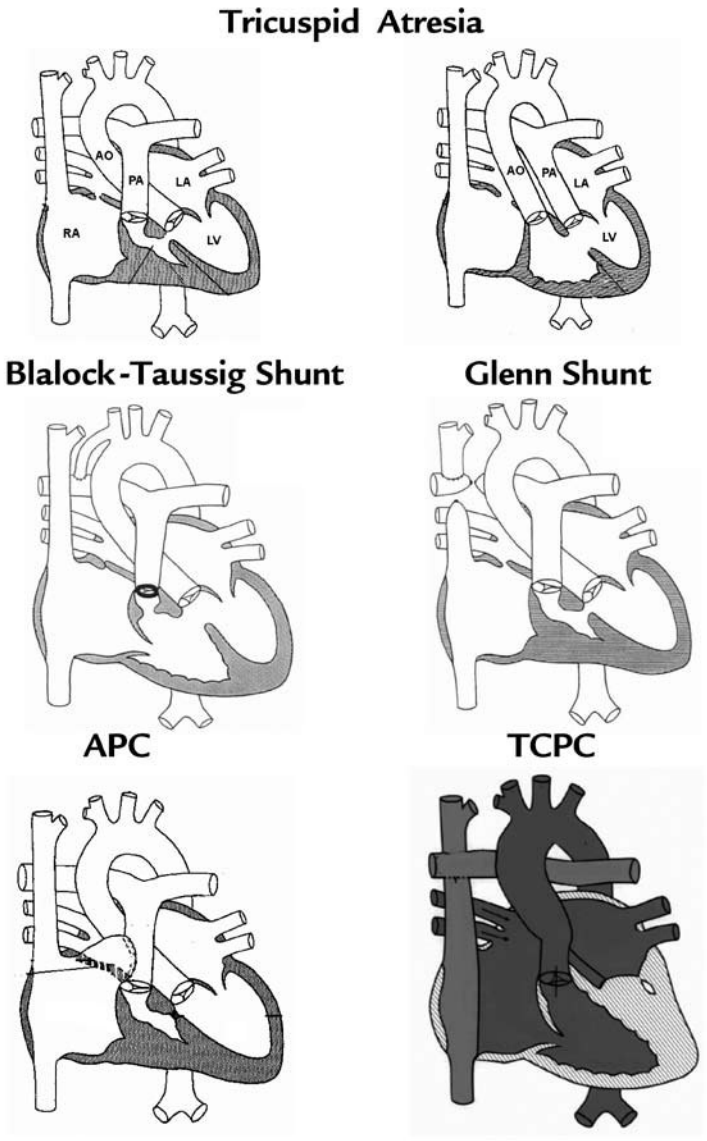

Figure 24.

Upper panel: tricuspid atresia is characterized by absence of the tricuspid valve and can be associated with normal position of the great arteries (left panel) or D-transposition of the great (right panel), an atrial septal defect or a ventricular septal defect. Middle panel: a Blalock-Taussig shunt connects one of the aortic branches, which usually is the subclavian artery, to the pulmonary artery; a Glenn shunt is a direct anastomosis between the superior caval vein and a pulmonary artery. Lower panel; APC: connection between the atrial (appendage) and the pulmonary trunk, TCPC: an end-to-side superior cavopulmonary anastomosis (bi-directional Glenn operation) combined with an intra-atrial tube connection of the inferior vena cava to the pulmonary arteries.
APC = direct atrio-pulmonary connection, TCPC = total cavopulmonary connection.

of this approach is that the left ventricle is restored as the systemic pump. Patients with congenital corrected transposition of the great arteries are repaired with a double-switch procedure: an atrial switch is combined with either an arterial switch procedure (absence of pulmonary stenosis) or a Rastelli-type repair (in case of pulmonary stenosis and ventricular septal defect, lower panel figure 23). As atrial switch procedures require a right atriotomy, an atrial septectomy and suture lines along the patches it is to be expected that atrial dysarrhythmias occur more frequently in patients who have had an atrial switch repair compared to patients with an arterial switch repair. Rhodes et al. indeed demonstrated that an arterial switch was associated with lower incidence of supraventricular tachycardias during long-term follow up (2.1 years).[198]

Tricuspid Atresia

Tricuspid atresia is characterized by absence of the tricuspid valve (upper panel Figure 24). Based upon the interrelationship of the great arteries, three different types can be distinguished; type I: normal position of the great arteries, type II: D-transposition of the great arteries, type III: L-transposition of the great arteries, type IV: persistent truncus arteriosus. Further subdivision of the different types of tricuspid atresia is made according to the presence of pulmonary valve pathology: subgroup A: pulmonary atresia, subgroup B: pulmonary stenosis, subgroup C: normal pulmonary arteries.

Most patients with tricuspid atresia require cardiac surgery in their first year of life. The aim of the surgical procedure is to connect the pulmonary and systemic circulation by constructing a shunt, e.g. a Blalock-Taussig shunt or a Glenn shunt (middle panel Figure 24).[199] The palliative surgical procedure for patients with tricuspid atresia is the Fontan procedure. A Fontan procedure is aimed at re-directing systemic venous blood directly into the pulmonary circulation without passing through the subpulmonary ventricle. The initial Fontan procedure consisted of the construction of 1) an end-to-end Glenn anastomose between the superior caval vein and the right pulmonary artery and 2) connection between the right atrium and the left pulmonary artery using an aortic homograft. Since then, several modifications have been made, e.g. direct atriopulmonary connection and total cavopulmonary (lateral tunnel) connection (lower panel figure 24).

Studies have demonstrated that risk factors for AT in patients with Fontan circulation include right atrial enlargement, elevated atrial pressure, dispersion of atrial refractoriness, sinus node dysfunction, older age at the time of cardiac surgery, elevation of pulmonary pressure, low aorta oxygen saturation, preoperative arrhythmias, a longer time after cardiac surgery.[200;201] Similar to the TGA patients, the surgical technique used is associated with the incidence of AT. Compared to the atriopulmonary connection, the cavopulmonary connection results in less right atrial pressure elevation and subsequent distension thereby reducing the incidence of late post-operative atrial arrhythmias. [201-206]

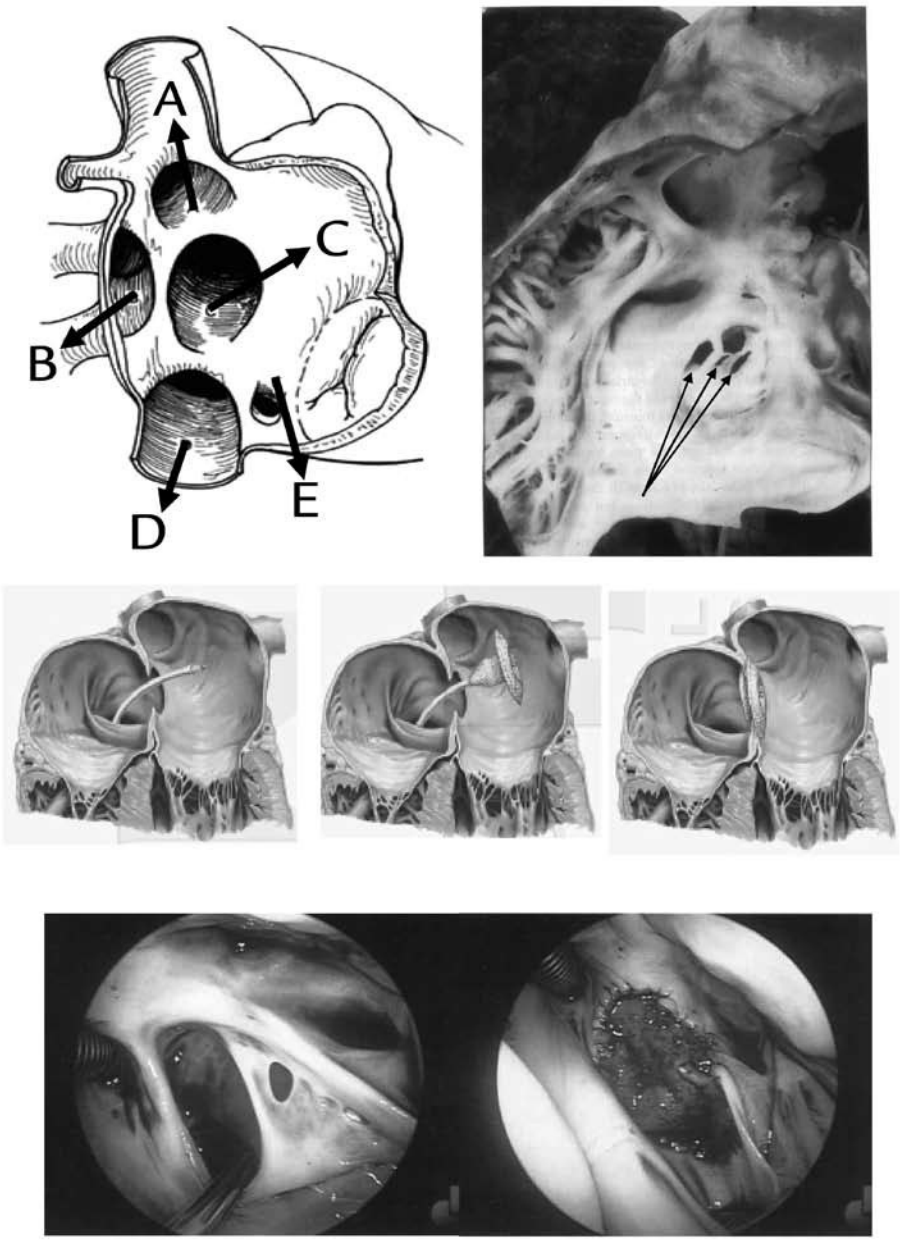

Figure 25.

Upper left panel: common sites of atrial septal defects. A = sinus venosus, B = posterior wall, C = fossa ovalis, D = inferior caval, E = coronary sinus. Upper right panel: atrial septum viewed from the right atrium demonstrating multiple fenestrations in the oval fossa. Middle panel: device closure of an atrial septal defect. Lower panel: patch closure of an atrial septal defect.

Atrial Septal Defect

Atrial septal defects (ASD) are defects of the ostium primum, ostium secundum, sinus venosus or coronary sinus (upper left panel **Figure 25**). The majority of the interatrial communications are ostium secundum defects (60-70%). An ostium secundum defect is an elliptical defect at the site of the foramen ovale in the midportion of the interatrial septum. This defect is the result of excessive resorption of the septum primum or deficient growth of the septum secundum. An ostium primum defect is a round defect low in the interatrial septum and is frequently associated with clefts of the mitral and tricuspid valves. Sinus venosus defects most often occur at the level of the superior caval vein with the atrial wall, resulting in a connection between the superior caval vein and both the right and left atrium. This type of defect is usually associated with anomalous drainage of the pulmonary veins. Sinus venosus defects at the level of the inferior caval vein are rare. Coronary sinus defects are right-to-left shunts between the coronary sinus wall and the left atrial wall and are also uncommon.

Surgical closure of ASD's requires a long anterior oblique atriotomy. The ASD is closed by a primary suture closure or by using a synthetic or pericardial patch (lower panel **Figure 25**). Transcatheter closures of ASD's are nowadays also frequently performed (middle panel **Figure 25**). The risk of developing atrial reentry tachycardias after surgical repair is associated with age at the time of the surgical repair, surgical modifications (e.g. cannulation techniques), pulmonary artery pressure, coexisting heart diseases and the presence of atrial arrhythmias before surgery.[168-170;207] Most common AT in patients with ASD are AFL and AF. Surgical closure does not prevent the occurrence of AFL and AF, particularly if patients are older than 40 years at the time of cardiac surgery.[169]

Morton et al. demonstrated that volume overload in patients with an ASD resulted in conduction delay at the terminal crest compared to age-matched control subjects.[208] After ASD closure, there was incomplete normalization of atrial size and persistence of conduction delay at the terminal crest. These findings suggest that impaired conduction at the terminal crest may be the substrate of late post-operative AT in this patient group.

Tetralogy of Fallot

The four cardiac abnormalities of the tetralogy of Fallot (ToF) are (sub)valvular pulmonary stenosis, large ventricular septal defect, right ventricular hypertrophy and an overriding aorta (left panel **Figure 26**).

Several palliative shunt operations for ToF have been developed, including the blalock Taussig, modified Blalock-Taussig, Potts (connection between the descending aorta and left pulmonary artery) and Waterston anastomosis (connection between the ascending aorta and right pulmonary artery). The Potts connection is shown in the middle panel of **Figure 26**. Repairative surgical treatment of ToF consists of closure of the ventricular septal defect with a patch and alleviation of the right ventricular outflow tract obstruction (right panel **Figure 26**). Surgical repair of ToF has been performed through either a

transatrial or transventricular approach. As the transatrial approach is associated with a reduced risk of ventricular arrhythmias, the transatrial approach is nowadays preferably used.[209] AT have been reported both after transventricular and transatrial repairs of ToF.[209] The incidence of AT is associated with pulmonary regurgitation, atrial volume overload, older age at the time of surgery or previous palliation with a Waterston or Potts anastomosis.[181;210;211]

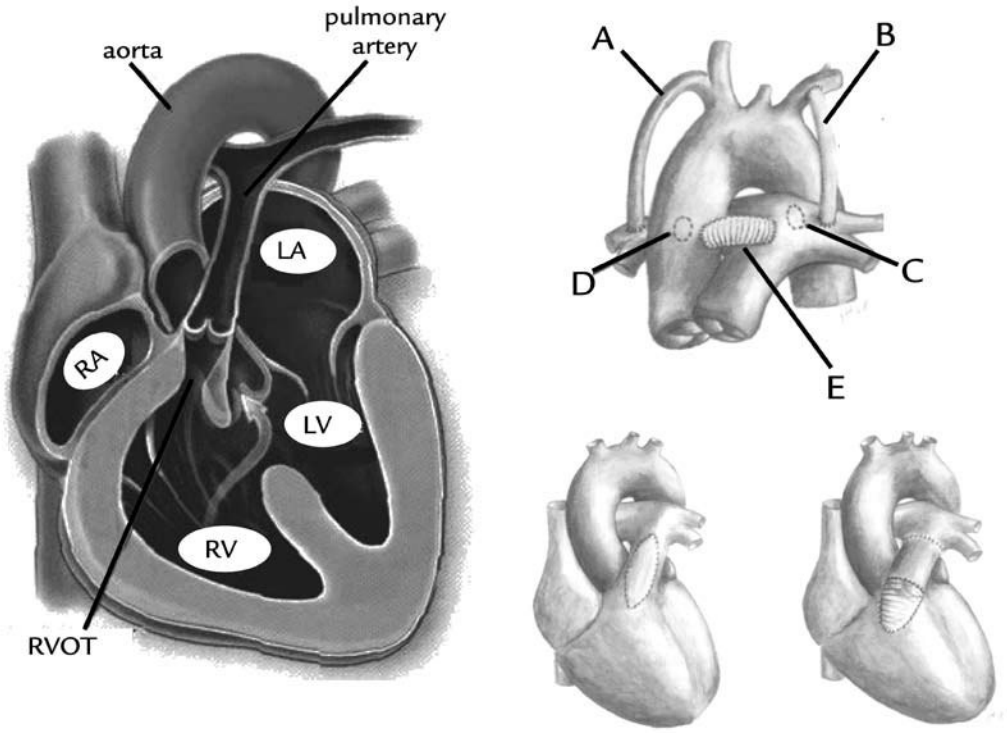

Figure 26.

Left panel: the four cardiac abnormalities of the tetralogy of Fallot (ToF) are (sub)valvular pulmonary stenosis, large ventricular septal defect, right ventricular hypertrophy and an overriding aorta. *Upper right panel:* several palliative shunt operations for ToF have been developed, including the blalock Taussig shunt (A, end-to-side anastomosis between the subclavian artery and the pulmonary trunk), a modified Blalock-Taussig shunt (B, gore-tex prothesis between the subclavian artery arteria subclavia and the ipsilateral pulmonary artery), a Potts shunt (C, connection between the descending aorta and left pulmonary artery), and Waterston shunt (D, connection between the ascending aorta and right pulmonary artery), a central shunt (E, a prosthetic tube between the ascending aorta and the pulmonary trunk). *Lower right panel:* repair of ToF with patch closure of the ventricular septal defect, pulmonary valvectomy and a right ventricular outflow- pulmonary trunk patch.

Outline of this thesis

Despite numerous reports on the outcome of different ablation approaches of AF, mapping studies performed in patients with AF are limited. As a consequence of the small number of mapping studies of human AF performed sofar, the exact mechanism underlying AF is still not completely understood. In **Chapter 1**, we discuss the outcome of mapping studies of both experimental and clinical AF in relation to the mechanism underlying AF.

In patients with chronic AF, spatial patterns of activation have never been examined nor has the relation between electrogram morphology and abnormalities in conduction been analyzed. Also, electrophysiological characteristics of different types of AF studied by high resolution mapping have never been compared. We therefore performed epicardial high density mapping studies during cardiac surgery in patients with induced AF and in patients with chronic AF in order to analyze differences in electro-physiological characteristics such as variation in fibrillation intervals, patterns of activation, heterogeneity in conduction and fractionation of fibrillation potentials (**Chapter 2 to 6**).

In order to individualize AF treatment, the mechanism of AF in each individual patient should be analyzed. For this purpose, multi-site high density mapping is required in order to identify focal sources or to localize areas of conduction abnormalities.
We evaluated a new epicardial multi-site high density mapping approach by performing total mapping of the atria with a so-called "finger-tip" electrode in patients with chronic AF. Epicardial mapping allows access to structures which can not be reached from the endocardial site such as Bachmann's bundle. In **Chapter 7**, we analyzed conduction characteristics of fibrillatory waves only at Bachmann's bundle. In **Chapter 8**, we assessed regional differences in various electrophysiological variables including fractionation of fibrillation potentials, variation in fibrillatory rate, heterogeneity in conduction and conduction anisotropy throughout the entire right and left atrium.

Mapping studies of regular AT in humans performed with recent developed sophisticated mapping techniques revealed that the mechanism underlying regular AT is more variable than expected and can most often not be predicted from the surface electrocardiogram.

Chapter 1 reviews mapping studies reporting on various macro-reentrant circuits underlying type I AFL. The results of these studies demonstrate that in the individual patient presenting with a "flutter-like" surface electrogram, 1) different types of reentrant circuits can be present and that 2) these macro-reentrant circuits are not always cavo-tricuspid isthmus dependent and ablative therapy aimed at creating a linear lesion across this corridor will therefore not be effective in eliminating the AT.

Catheter ablation studies have described fractionated electrograms at successful ablation sites of reentry AT. As fractionated electrograms are recorded from areas where conduction is dissociated, they could theoretically be regarded as indicators of the arrhythmogenic substrate. Mapping of AT in order to study electrogram morphology and corresponding patterns of activation are therefore essential in order to comprehend genesis and perpetuation of tachyarrhythmias.
In clinical practice, mapping of AT is particularly challenging in patients with post-operative AT. Distorted, dilated atria due cardiac surgery, progressive atrial scarring as a result of hemodynamic overload and the presence of prosthetic material all increase the complexity of the arrhythmogenic substrate. Mapping of these post-operative AT is facilitated by using 3-dimensional electro-anatomical mapping systems as they visualize the reentry circuit in a 3-dimensonal reconstruction of the atria (**Chapter 9 and 15**).
In **Chapter 10 and 11**, endocardial 3-dimensional electro-anatomical sequential mapping techniques were used to map AT in humans. Voltage maps were constructed in patients with congenital heart disease and compared with voltage maps obtained from patients with normal atria. From these studies, a cut-off value was defined for discriminating 'healthy' from 'diseased' myocardium in order to facilitate identification of the arrhythmogenic substrate in subjects with congenital heart disease. By applying these mapping criteria, the mechanism underlying late post-operative AT was studied in a large cohort of patients with congenital heart disease (**Chapter 12**).

In **Chapter 13,** we evaluated the assumption that arising of a focal AT requires a poor cell-to-cell coupling. For this purpose, endocardial 3-dimensional electro-anatomical activation mapping during focal AT was performed in patients with normal atria and in patients with previous cardiac surgery for either congenital heart defects or acquired valvular disease. The incidence of fractionated atrial electrograms at the focal AT origin was determined and characteristics of atrial electrograms in relation to their distance to the site of earliest activity during focal AT were studied.

References

1. Peters NS, Schilling RJ, Kanagaratnam P et al. Atrial fibrillation: strategies to control, combat, and cure. Lancet. 2002;359:593-603.
2. Levy S. Epidemiology and classification of atrial fibrillation. J Cardiovasc Electrophysiol. 1998;9:S78-S82.
3. Psaty BM, Manolio TA, Kuller LH et al. Incidence of and risk factors for atrial fibrillation in older adults. Circulation. 1997;96:2455-2461.
4. Kannel WB, Abbott RD, Savage DD et al. Epidemiologic features of chronic atrial fibrillation: the Framingham study. N Engl J Med. 1982;306:1018-1022.
5. Knight BP. Atrial fibrillation in patients with congestive heart failure. Pacing Clin Electrophysiol. 2003;26:1620-1623.
6. Levy S. Epidemiology and classification of atrial fibrillation. J Cardiovasc Electrophysiol. 1998;9:S78-S82.
7. Blaauw Y, Van Gelder IC, Crijns HJ. Treatment of atrial fibrillation. Heart. 2002;88:432-437.
8. Padanilam BJ, Prystowsky EN. Should atrial fibrillation ablation be considered first-line therapy for some patients? Should ablation be first-line therapy and for whom? the antagonist position. Circulation. 2005;112:1223-1229.
9. Verma A, Natale A. Should atrial fibrillation ablation be considered first-line therapy for some patients? Why atrial fibrillation ablation should be considered first-line therapy for some patients. Circulation. 2005;112:1214-1222.
10. Scheinman MM, Morady F. Nonpharmacological approaches to atrial fibrillation. Circulation. 2001;103:2120-2125.
11. Markides V, Schilling RJ. Atrial fibrillation: classification, pathophysiology, mechanisms and drug treatment. Heart. 2003;89:939-943.
12. Gepstein L, Hayam G, Ben Haim SA. A novel method for nonfluoroscopic catheter-based electroanatomical mapping of the heart. In vitro and in vivo accuracy results. Circulation. 1997;95:1611-1622.
13. Gepstein L, Evans SJ. Electroanatomical mapping of the heart: basic concepts and implications for the treatment of cardiac arrhythmias. Pacing Clin Electrophysiol. 1998;21:1268-1278.
14. Schalij MJ, van Rugge FP, Siezenga M et al. Endocardial activation mapping of ventricular tachycardia in patients – First application of a 32-site bipolar mapping electrode catheter. Circulation. 1998;98:2168-2179.
15. Schilling RJ, Kadish AH, Peters NS et al. Endocardial mapping of atrial fibrillation in the human right atrium using a non-contact catheter. Eur Heart J. 2000;21:550-564.
16. Wittkampf FH, Wever EF, Derksen R et al. LocaLisa: new technique for real-time 3-dimensional localization of regular intracardiac electrodes. Circulation. 1999;99:1312-1317.
17. Wittkampf FH, Wever EF, Derksen R et al. Accuracy of the LocaLisa system in catheter ablation procedures. J Electrocardiol. 1999;32 Suppl:7-12.
18. Zipes DP. Mechanisms of clinical arrhythmias. J Cardiovasc Electrophysiol. 2003;14:902-912.
19. Khaja A, Flaker G. Bachmann's bundle: does it play a role in atrial fibrillation? Pacing Clin Electrophysiol. 2005;28:855-863.
20. Kucera JP, Rudy Y. Mechanistic insights into very slow conduction in branching cardiac tissue: a model study. Circ Res. 2001;89:799-806.
21. Sanchez-Quintana D, Anderson RH, Cabrera JA et al. The terminal crest: morphological features relevant to electrophysiology. Heart. 2002;88:406-411.
22. Tan AY, Chou CC, Zhou S et al. Electrical Connections Between the Left Superior Pulmonary Vein, Left Atrium and Ligament of Marshall: Implications for the Mechanisms of Atrial Fibrillation. Am J Physiol Heart Circ Physiol. 2005.
23. Volkmer M, Antz M, Hebe J et al. Focal atrial tachycardia originating from the musculature of the coronary sinus. J Cardiovasc Electrophysiol. 2002;13:68-71.
24. Cox JL, Canavan TE, Schuessler RB et al. The surgical treatment of atrial fibrillation. II. Intraoperative electrophysiologic mapping and description of the electrophysiologic basis of atrial flutter and atrial fibrillation. J Thorac Cardiovasc Surg. 1991;101:406-426.

25. Spach MS. Transition from a continuous to discontinuous understanding of cardiac conduction. Circ Res. 2003;92:125-126.
26. Spach MS, Dolber PC. Relating extracellular potentials and their derivatives to anisotropic propagation at a microscopic level in human cardiac muscle. Evidence for electrical uncoupling of side-to-side fiber connections with increasing age. Circ Res. 1986;58:356-371.
27. Spach MS. Anisotropy of cardiac tissue: a major determinant of conduction? J Cardiovasc Electrophysiol. 1999;10:887-890.
28. Spach MS, Heidlage JF, Dolber PC et al. Electrophysiological effects of remodeling cardiac gap junctions and cell size: experimental and model studies of normal cardiac growth. Circ Res. 2000;86:302-311.
29. Spach MS, Barr RC. Effects of cardiac microstructure on propagating electrical waveforms. Circ Res. 2000;86:E23-E28.
30. Spach MS. The discontinuous nature of electrical propagation in cardiac muscle. Consideration of a quantitative model incorporating the membrane ionic properties and structural complexities. The ALZA distinguished lecture. Ann Biomed Eng. 1983;11:209-261.
31. Spach MS, Heidlage JF, Barr RC et al. Cell size and communication: role in structural and electrical development and remodeling of the heart. Heart Rhythm. 2004;1:500-515.
32. Ho SY, Anderson RH, Sanchez-Quintana D. Gross structure of the atriums: More than an anatomic curiosity? Pace-Pacing and Clinical Electrophysiology. 2002;25:342-350.
33. Ho SY, Anderson RH, Sanchez-Quintana D. Atrial structure and fibres: morphologic bases of atrial conduction. Cardiovascular Research. 2002;54:325-336.
34. Cabo C, Pertsov AM, Baxter WT et al. Wave-front curvature as a cause of slow conduction and block in isolated cardiac muscle.
35. Spach MS, Miller WT, III, Dolber PC et al. The functional role of structural complexities in the propagation of depolarization in the atrium of the dog. Cardiac conduction disturbances due to discontinuities of effective axial resistivity. Circ Res. 1982;50:175-191.
36. Kalman JM, Olgin JE, Karch MR et al. "Cristal tachycardias": origin of right atrial tachycardias from the crista terminalis identified by intracardiac echocardiography. J Am Coll Cardiol. 1998;31:451-459.
37. Joyner RW. Modulation of repolarization by electrotonic interactions. Jpn Heart J. 1986;27 Suppl 1:167-183.
38. Joyner RW, Wang YG, Wilders R et al. A spontaneously active focus drives a model atrial sheet more easily than a model ventricular sheet. Am J Physiol Heart Circ Physiol. 2000;279:H752-H763.
39. Wagner MB, Golod D, Wilders R et al. Modulation of propagation from an ectopic focus by electrical load and by extracellular potassium. Am J Physiol. 1997;272:H1759-H1769.
40. Olgin JE, Kalman JM, Fitzpatrick AP et al. Role of right atrial endocardial structures as barriers to conduction during human type I atrial flutter. Activation and entrainment mapping guided by intracardiac echocardiography. Circulation. 1995;92:1839-1848.
41. Matsuo K, Uno K, Khrestian CM et al. Conduction left-to-right and right-to-left across the crista terminalis. American Journal of Physiology-Heart and Circulatory Physiology. 2001;280:H1683-H1691.
42. Gray RA, Pertsov AM, Jalife J. Incomplete reentry and epicardial breakthrough patterns during atrial fibrillation in the sheep heart. Circulation. 1996;94:2649-2661.
43. Hassink RJ, Aretz HT, Ruskin J et al. Morphology of atrial myocardium in human pulmonary veins: a postmortem analysis in patients with and without atrial fibrillation. J Am Coll Cardiol. 2003;42:1108-1114.
44. Perez-Lugones A, McMahon JT, Ratliff NB et al. Evidence of specialized conduction cells in human pulmonary veins of patients with atrial fibrillation. J Cardiovasc Electrophysiol. 2003;14:803-809.
45. Kato R, Lickfett L, Meininger G et al. Pulmonary vein anatomy in patients undergoing catheter ablation of atrial fibrillation: lessons learned by use of magnetic resonance imaging. Circulation. 2003;107:2004-2010.
46. Ho SY, Cabrera JA, Tran VH et al. Architecture of the pulmonary veins: relevance to radiofrequency ablation. Heart. 2001;86:265-270.

47. Tagawa M, Higuchi K, Chinushi M et al. Myocardium extending from the left atrium onto the pulmonary veins: a comparison between subjects with and without atrial fibrillation. Pacing Clin Electrophysiol. 2001;24:1459-1463.
48. Schwartzman D, Lacomis J, Wigginton WG. Characterization of left atrium and distal pulmonary vein morphology using multidimensional computed tomography. J Am Coll Cardiol. 2003;41:1349-1357.
49. Hocini M, Ho SY, Kawara T et al. Electrical conduction in canine pulmonary veins: electrophysiological and anatomic correlation. Circulation. 2002;105:2442-2448.
50. Fynn SP, Kalman JM. Pulmonary veins: anatomy, electrophysiology, tachycardia, and fibrillation. Pacing Clin Electrophysiol. 2004;27:1547-1559.
51. Hamabe A, Okuyama Y, Miyauchi Y et al. Correlation between anatomy and electrical activation in canine pulmonary veins. Circulation. 2003;107:1550-1555.
52. Chen SA, Chen YJ, Yeh HI et al. Pathophysiology of the pulmonary vein as an atrial fibrillation initiator: From bench to clinic. Pace-Pacing and Clinical Electrophysiology. 2003;26:1576-1582.
53. Chen SA, Hsieh MH, Tai CT et al. Initiation of atrial fibrillation by ectopic beats originating from the pulmonary veins: electrophysiological characteristics, pharmacological responses, and effects of radiofrequency ablation. Circulation. 1999;100:1879-1886.
54. Arora R, Verheule S, Scott L et al. Arrhythmogenic substrate of the pulmonary veins assessed by high-resolution optical mapping. Circulation. 2003;107:1816-1821.
55. Kumagai K, Uno K, Khrestian C et al. Single site radiofrequency catheter ablation of atrial fibrillation: Studies guided by simultaneous multisite mapping in the canine sterile pericarditis model. Journal of the American College of Cardiology. 2000;36:917-923.
56. Lemery R, Guiraudon G, Veinot JP. Anatomic description of Bachmann's bundle and its relation to the atrial septum. American Journal of Cardiology. 2003;91:1482-1485.
57. Kumagai K, Khrestian C, Waldo AL. Simultaneous multisite mapping studies during induced atrial fibrillation in the sterile pericarditis model. Insights into the mechanism of its maintenance. Circulation. 1997;95:511-521.
58. O'Donnell D, Bourke JP, Furniss SS. Interatrial transseptal electrical conduction: comparison of patients with atrial fibrillation and normal controls. J Cardiovasc Electrophysiol. 2002;13:1111-1117.
59. Becker AE. How structurally normal are human atria in patients with atrial fibrillation ? Heart Rhythm 1, 627-631.
60. Chauvin M, Shah DC, Haissaguerre M et al. The anatomic basis of connections between the coronary sinus musculature and the left atrium in humans. Circulation. 2000;101:647-652.
61. Nair M, Shah P, Batra R et al. Chronic atrial fibrillation in patients with rheumatic heart disease – Mapping and radiofrequency ablation of flutter circuits seen at initiation after cardioversion. Circulation. 2001;104:802-809.
62. Oral H, Ozaydin M, Chugh A et al. Role of the coronary sinus in maintenance of atrial fibrillation. J Cardiovasc Electrophysiol. 2003;14:1329-1336.
63. Eckardt L. Automaticity in the coronary sinus. J Cardiovasc Electrophysiol. 2002;13:288-289.
64. Antz M, Otomo K, Arruda M et al. Electrical conduction between the right atrium and the left atrium via the musculature of the coronary sinus. Circulation. 1998;98:1790-1795.
65. Frustaci A, Chimenti C, Bellocci F et al. Histological substrate of atrial biopsies in patients with lone atrial fibrillation. Circulation. 1997;96:1180-1184.
66. Kostin S, Klein G, Szalay Z et al. Structural correlate of atrial fibrillation in human patients. Cardiovascular Research. 2002;54:361-379.
67. Koura T, Hara M, Takeuchi S et al. Anisotropic conduction properties in canine atria analyzed by high-resolution optical mapping: preferential direction of conduction block changes from longitudinal to transverse with increasing age. Circulation. 2002;105:2092-2098.
68. Boldt A, Wetzel U, Lauschke J et al. Fibrosis in left atrial tissue of patients with atrial fibrillation with and without underlying mitral valve disease. Heart. 2004;90:400-405.
69. Corradi D, Callegari S, Benussi S et al. Regional left atrial interstitial remodeling in patients with chronic atrial fibrillation undergoing mitral-valve surgery. Virchows Arch. 2004;445:498-505.
70. Carver W, Nagpal ML, Nachtigal M et al. Collagen expression in mechanically stimulated cardiac fibroblasts. Circ Res. 1991;69:116-122.
71. Berbari EJ, Landr P, Geselowitz DB. The methodology of cardiac mapping. 1993: 11-134.

72. de Groot NM, Bootsma M, van der Velde ET et al. Three-dimensional catheter positioning during radiofrequency ablation in patients: First application of a real-time position management system. Journal of Cardiovascular Electrophysiology. 2000;11:1183-1192.
73. de Groot NMS, van der Burg AEB, Bootsma M et al. The use of the dynamic deformable heart chamber model facilitates catheter ablation of atrial flutter: a novel endocardial mapping technique based on the 3D real-time positioning management system. European Heart Journal. 2001;22:180.
74. Zrenner B, Ndrepepa G, Schneider M et al. Basket catheter-guided three-dimensional activation patterns construction and ablation of common type atrial flutter. Pace-Pacing and Clinical Electrophysiology. 2000;23:1350-1358.
75. de Groot NMS, van Erven L, Kuijper AFM et al. Endocardial mapping and catheter ablation of atrial flutter using a 32-bipolar basket catheter. American Journal of Cardiology. 1999;84:121P-122P.
76. de Groot NMS, Kuijper AFM, van Erven L et al. Radiofrequency ablation of ventricular tachycardia guided by a steerable high density sector basket catheter. Circulation. 1999;100:289.
77. Spach MS, Kootsey JM. Relating the sodium current and conductance to the shape of transmembrane and extracellular potentials by simulation: effects of propagation boundaries. IEEE Trans Biomed Eng. 1985;32:743-755.
78. Durrer D, van der Twell LH. Spread of activation in the left ventricular wall of the dog. I. Am Heart J. 1953;46:683-691.
79. Biermann M, Shenasa M, Borggrefe N et al. The interpretation of cardiac electrograms. Cardiac mapping. New York: Futura Publishing, 1993: 11-31.
80. Bakker J, Hauer R, Simmers T. Activation time mapping: unipolar versus bipolar recording. Cardiac electrophysiology from cell to bedside. Philadelphia: WB Saunders Company, 1995: 1068-1078.
81. Spach MS, Kootsey JM. Relating the sodium current and conductance to the shape of transmembrane and extracellular potentials by simulation: effects of propagation boundaries. IEEE Trans Biomed Eng. 1985;32:743-755.
82. Cosio FG. Atrial flutter update. Card Electrophysiol Rev. 2002;6:356-364.
83. Wells JL, Jr., MacLean WA, James TN et al. Characterization of atrial flutter. Studies in man after open heart surgery using fixed atrial electrodes. Circulation. 1979;60:665-673.
84. Waldo AL. Treatment of atrial flutter. Heart. 2000;84:227-232.
85. Cosio FG, Goicolea A, Lopez-Gil M et al. Catheter ablation of atrial flutter circuits. Pacing Clin Electrophysiol. 1993;16:637-642.
86. Cosio FG. Atrial flutter update. Card Electrophysiol Rev. 2002;6:356-364.
87. Cosio FG, Martin-Penato A, Pastor A et al. Atypical flutter: a review. Pacing Clin Electrophysiol. 2003;26:2157-2169.
88. Della Bella P, Fraticelli A, Tondo C et al. Atypical atrial flutter: clinical features, electrophysiological characteristics and response to radiofrepuency catheter ablation. Europace. 2002;4:241-253.
89. Lee KW, Yang Y, Scheinman MM. Atrial flutter: a review of its history, mechanisms, clinical features, and current therapy. Curr Probl Cardiol. 2005;30:121-167.
90. Ricard P, Imianitoff M, Yaici K et al. Atypical atrial flutters. Europace. 2002;4:229-239.
91. Schmitt C, Ndrepepa G, Zrenner B. Reentry circuit location and left atrial three-dimensional activation patterns in left atrial flutter. Zeitschrift fur Kardiologie. 2001;90:292-296.
92. Shah D, Jais P, Takahashi A et al. Dual-loop intra-atrial reentry in humans. Circulation. 2000;101:631-639.
93. Tai CT, Lin YK, Chen SA. Atypical atrial flutter involving the isthmus between the right pulmonary veins and fossa ovalis. Pace-Pacing and Clinical Electrophysiology. 2001;24:384-387.
94. Cheng J, Cabeen WR, Scheinman MM. Right atrial flutter due to lower loop reentry – Mechanism and anatomic substrates. Circulation. 1999;99:1700-1705.
95. Cosio FG. Atrial flutter update. Card Electrophysiol Rev. 2002;6:356-364.
96. Milliez P, Richardson AW, Obioha-Ngwu O et al. Variable electrocardiographic characteristics of isthmus-dependent atrial flutter. J Am Coll Cardiol. 2002;40:1125-1132.
97. Chen J, de Chillou C, Hoff PI et al. Identification of extremely slow conduction in the cavotricuspid isthmus during common atrial flutter ablation. Journal of Interventional Cardiac Electrophysiology. 2002;7:67-75.
98. Kalman JM, Olgin JE, Saxon LA et al. Activation and entrainment mapping defines the tricuspid annulus as the anterior barrier in typical atrial flutter. Circulation. 1996;94:398-406.

99. Olgin JE, Kalman JM, Saxon LA et al. Mechanism of initiation of atrial flutter in humans: site of unidirectional block and direction of rotation. J Am Coll Cardiol. 1997;29:376-384.
100. Olshansky B, Okumura K, Hess PG et al. Demonstration of An Area of Slow Conduction in Human Atrial-Flutter. Journal of the American College of Cardiology. 1990;16:1639-1648.
101. Waldo AL. Pathogenesis of atrial flutter. J Cardiovasc Electrophysiol. 1998;9:S18-S25.
102. Yang YF, Cheng J, Bochoeyer A et al. Atypical right atrial flutter patterns Circulation. 2001;103:3092-3098.
103. Ricard P, Imianitoff M, Yaici K et al. Atypical atrial flutters. Europace. 2002;4:229-239.
104. Jais P, Shah DC, Haissaguerre M et al. Mapping and ablation of left atrial flutters. Circulation. 2000;101:2928-2934.
105. Jais P, Hocini M, Weerasoryia R et al. Atypical left atrial flutters. Card Electrophysiol Rev. 2002;6:371-377.
106. Scheinman MM, Cheng J, Yang Y. Mechanisms and clinical implications of atypical atrial flutter. J Cardiovasc Electrophysiol. 1999;10:1153-1157.
107. Ouyang FF, Ernst S, Vogtmann T et al. Characterization of reentrant circuits in left atrial macroreentrant tachycardia – Critical isthmus block can prevent atrial tachycardia recurrence. Circulation. 2002;105:1934-1942.
108. Bochoeyer A, Yang YF, Cheng J et al. Surface electrocardiographic characteristics of right and left atrial flutter. Circulation. 2003;108:60-66.
109. Marrouche NF, Natale A, Wazni OM et al. Left septal atrial flutter: electrophysiology, anatomy, and results of ablation. Circulation. 2004;109:2440-2447.
110. Kalman JM, VanHare GF, Olgin JE et al. Ablation of 'incisional' reentrant atrial tachycardia complicating surgery for congenital heart disease. Use of entrainment to define a critical isthmus of conduction. Circulation. 1996;93:502-512.
111. Walsh EP. Arrhythmias in patients with congenital heart disease. Card Electrophysiol Rev. 2002;6:422-430.
112. Saoudi N, Cosio F, Waldo A et al. A classification of atrial flutter and regular atrial tachycardia according to electrophysiological mechanisms and anatomical bases – A statement from a Joint Expert Group from the Working Group of Arrhythmias of the European Society of Cardiology and the North American Society of Pacing and electrophysiology. European Heart Journal. 2001;22:1162-1182.
113. Higa S, Tai CT, Lin YJ et al. Mechanism of adenosine-induced termination of focal atrial tachycardia. J Cardiovasc Electrophysiol. 2004;15:1387-1393.
114. Markowitz SM, Brodman RF, Stein KM et al. Lesional tachycardias related to mitral valve surgery. J Am Coll Cardiol. 2002;39:1973-1983.
115. Kistler PM, Sanders P, Hussin A et al. Focal atrial tachycardia arising from the mitral annulus – Electrocardiographic and electrophysiologic characterization. Journal of the American College of Cardiology. 2003;41:2212-2219.
116. Chen SA, Tai CT, Chiang CE et al. Focal atrial tachycardia: reanalysis of the clinical and electrophysiologic characteristics and prediction of successful radiofrequency ablation. J Cardiovasc Electrophysiol. 1998;9:355-365.
117. Engelstein ED, Lippman N, Stein KM et al. Mechanism-specific effects of adenosine on atrial tachycardia. Circulation. 1994;89:2645-2654.
118. Markowitz SM, Stein KM, Mittal S et al. Differential effects of adenosine on focal and macroreentrant atrial tachycardia. J Cardiovasc Electrophysiol. 1999;10:489-502.
119. Kammeraad JAE, Balaji S, Oliver RP et al. Nonautomatic focal atrial tachycardia: Characterization and ablation of a poorly understood arrhythmia in 38 patients. Pace-Pacing and Clinical Electrophysiology. 2003;26:736-742.
120. Higa S, Tai CT, Lin YJ et al. Focal atrial tachycardia: new insight from noncontact mapping and catheter ablation. Circulation. 2004;109:84-91.
121. Schmitt H, Weber S, Schwab JO et al. Diagnosis and ablation of focal right atrial tachycardia using a new nigh-resolution, non-contact mapping system. American Journal of Cardiology. 2001;87:1017-+.
122. Wetzel U, Hindricks G, Schirdewahn P et al. A stepwise mapping approach for localization and ablation of ectopic right, left, and septal atrial foci using electroanatomic mapping. European Heart Journal. 2002;23:1387-1393.

123. Hoffmann E, Reitmann C, Nimmermann P et al. Clinical experience with electroanatomic mapping of ectopic atrial tachycardia. Pace-Pacing and Clinical Electrophysiology. 2002;25:49-56.
124. Weiss C, Willems S, Rueppel R et al. Electroanatomical mapping (CARTO (R)) of ectopic atrial tachycardia: Impact of bipolar and unipolar local electrogram annotation for localization the focal origin Journal of Interventional Cardiac Electrophysiology. 2001;5:101-107.
125. Schmitt C, Zrenner B, Schneider M et al. Clinical experience with a novel multielectrode basket catheter in right atrial tachycardias. Circulation. 1999;99:2414-2422.
126. Lesh MD, Van Hare GF. Status of ablation in patients with atrial tachycardia and flutter. Pacing Clin Electrophysiol. 1994;17:1026-1033.
127. Lesh MD, Van Hare GF, Epstein LM et al. Radiofrequency catheter ablation of atrial arrhythmias. Results and mechanisms. Circulation. 1994;89:1074-1089.
128. Moe GK, Abilskov JA. Atrial fibrillation as a self-sustaining arrhythmia independent of focal discharge. Am Heart J. 1959;58:59-70.
129. Moe GK, Rheinboldt WC, Abildskov JA. A computer model of atrial fibrillation. Am Heart J. 1964;67:200-220.
130. Allessie MA, Lammers W.J.E.P, Bonke F.I.M et al. Experimental evaluation of Moe's multiple wavelet hypothesis of atrial fibrillation. In: D P Zipes and J Jalife (eds)- Cardiac Arrhythmias. 1985;Grune&Stratton, New York:265-276.
131. Konings KT, Kirchhof CJ, Smeets JR et al. High-density mapping of electrically induced atrial fibrillation in humans. Circulation. 1994;89:1665-1680.
132. Schuessler RB, Kawamoto T, Hand DE et al. Simultaneous epicardial and endocardial activation sequence mapping in the isolated canine right atrium. Circulation. 1993;88:250-263.
133. Derakhchan K, Li D, Courtemanche M et al. Method for simultaneous epicardial and endocardial mapping of in vivo canine heart: application to atrial conduction properties and arrhythmia mechanisms. J Cardiovasc Electrophysiol. 2001;12:548-555.
134. Skanes AC, Mandapati R, Berenfeld O et al. Spatiotemporal periodicity during atrial fibrillation in the isolated sheep heart.
135. Berenfeld O, Mandapati R, Dixit S et al. Spatially distributed dominant excitation frequencies reveal hidden organization in atrial fibrillation in the Langendorff-perfused sheep heart. J Cardiovasc Electrophysiol. 2000;11:869-879.
136. Mandapati R, Skanes A, Chen J et al. Stable microreentrant sources as a mechanism of atrial fibrillation in the isolated sheep heart. Circulation. 2000;101:194-199.
137. Gerstenfeld EP, Sahakian AV, Swiryn S. Evidence for Transient Linking of Atrial Excitation During Atrial-Fibrillation in Humans. Circulation. 1992;86:375-382.
138. Schoenwald AT, Sahakian AV, Swiryn S. Discrimination of atrial fibrillation from regular atrial rhythms by spatial precision of local activation direction. IEEE Trans Biomed Eng. 1997;44:958-963.
139. Chen J, Mandapati R, Berenfeld O et al. Dynamics of wavelets and their role in atrial fibrillation in the isolated sheep heart. Cardiovasc Res. 2000;48:220-232.
140. Okuyama Y, Miyauchi Y, Park AM et al. High resolution mapping of the pulmonary vein and the vein of Marshall during induced atrial fibrillation and atrial tachycardia in a canine model of pacing-induced congestive heart failure. J Am Coll Cardiol. 2003;42:348-360.
141. Harada A, Sasaki K, Fukushima T et al. Atrial activation during chronic atrial fibrillation in patients with isolated mitral valve disease. Ann Thorac Surg. 1996;61:104-111.
142. Harada A, Konishi T, Fukata M et al. Intraoperative map guided operation for atrial fibrillation due to mitral valve disease. Ann Thorac Surg. 2000;69:446-450.
143. Sueda T, Nagata H, Shikata H et al. Simple left atrial procedure for chronic atrial fibrillation associated with mitral valve disease. Ann Thorac Surg. 1996;62:1796-1800.
144. Holm M, Johansson R, Brandt J et al. Epicardial right atrial free wall mapping in chronic atrial fibrillation. Documentation of repetitive activation with a focal spread--a hitherto unrecognised phenomenon in man. Eur Heart J. 1997;18:290-310.
145. Nitta T, Ishii Y, Miyagi Y et al. Concurrent multiple left atrial focal activations with fibrillatory conduction and right atrial focal or reentrant activation as the mechanism in atrial fibrillation. J Thorac Cardiovasc Surg. 2004;127:770-778.
146. Sahadevan J, Ryu K, Peltz L et al. Epicardial mapping of chronic atrial fibrillation in patients: preliminary observations. Circulation. 2004;110:3293-3299.

147. Sih HJ, Zipes DP, Berbari EJ et al. A high-temporal resolution algorithm for quantifying organization during atrial fibrillation. IEEE Trans Biomed Eng. 1999;46:440-450.
148. Akar JG, Everett TH, Kok LC et al. Effect of electrical and structural remodeling on spatiotemporal organization in acute and persistent atrial fibrillation. Journal of Cardiovascular Electrophysiology. 2002;13:1027-1034.
149. Niwano S, Aizawa Y. Fragmented atrial activity in patients with transient atrial fibrillation. Am Heart J. 1991;121:62-67.
150. Shimizu A, Fukatani M, Tanigawa M et al. Intra-atrial conduction delay and fragmented atrial activity in patients with paroxysmal atrial fibrillation Jpn Circ J. 1989;53:1023-1030.
151. Centurion OA, Fukatani M, Konoe A et al. Different Distribution of Abnormal Endocardial Electrograms Within the Right Atrium in Patients with Sick Sinus Syndrome. British Heart Journal. 1992;68:596-600.
152. Tanigawa M, Fukatani M, Konoe A et al. Prolonged and Fractionated Right Atrial Electrograms During Sinus Rhythm in Patients with Paroxysmal Atrial-Fibrillation and Sick Sinus Node Syndrome. Journal of the American College of Cardiology. 1991;17:403-408.
153. Nakao K, Seto S, Ueyama C et al. Extended distribution of prolonged and fractionated right atrial electrograms predicts the development of chronic atrial fibrillation in patients with idiopathic paroxysmal atrial fibrillation. Journal of the American College of Cardiology. 2002;39:116A.
154. Wells JL, Jr., Karp RB, Kouchoukos NT et al. Characterization of atrial fibrillation in man: studies following open heart surgery. Pacing Clin Electrophysiol. 1978;1:426-438.
155. Li W, Somerville J. Atrial flutter in grown-up congenital heart (GUCH) patients. Clinical characteristics of affected population. Int J Cardiol. 2000;75:129-137.
156. Shan Z, Van Der Voort PH, Blaauw Y et al. Fractionation of electrograms and linking of activation during pharmacologic cardioversion of persistent atrial fibrillation in the goat. J Cardiovasc Electrophysiol. 2004;15:572-580.
157. Jais P, Haissaguerre M, Shah DC et al. Regional disparities of endocardial atrial activation in paroxysmal atrial fibrillation. Pacing Clin Electrophysiol. 1996;19:1998-2003.
158. Konings KT, Smeets JL, Penn OC et al. Configuration of unipolar atrial electrograms during electrically induced atrial fibrillation in humans. Circulation. 1997;95:1231-1241.
159. Kuck KH, Ernst S, Cappato R et al. Nonfluoroscopic endocardial catheter mapping of atrial fibrillation. J Cardiovasc Electrophysiol. 1998;9:S57-S62.
160. Nademanee K, McKenzie J, Kosar E et al. A new approach for catheter ablation of atrial fibrillation: mapping of the electrophysiologic substrate. J Am Coll Cardiol. 2004;43:2044-2053.
161. Pachon MJ, Pachon ME, Pachon MJ et al. A new treatment for atrial fibrillation based on spectral analysis to guide the catheter RF-ablation. Europace. 2004;6:590-601.
162. Bender HW, Jr., Stewart JR, Merrill WH et al. Ten years' experience with the Senning operation for transposition of the great arteries: physiological results and late follow-up. Ann Thorac Surg. 1989;47:218-223.
163. Haines DE, DiMarco JP. Sustained intraatrial reentrant tachycardia: clinical, electrocardiographic and electrophysiologic characteristics and long-term follow-up. J Am Coll Cardiol. 1990;15:1345-1354.
164. Lan YT, Lee JC, Wetzel G. Postoperative arrhythmia. Curr Opin Cardiol. 2003;18:73-78.
165. Vetter VL, Horowitz LN. Electrophysiologic residua and sequelae of surgery for congenital heart defects. Am J Cardiol. 1982;50:588-604.
166. Peters NS, Somerville J. Arrhythmias after the Fontan procedure. Br Heart J. 1992;68:199-204.
167. Triedman JK. Arrhythmias in adults with congenital heart disease. Heart. 2002;87:383-389.
168. Brandenburg RO, Jr., Holmes DR, Jr., Brandenburg RO et al. Clinical follow-up study of paroxysmal supraventricular tachyarrhythmias after operative repair of a secundum type atrial septal defect in adults. Am J Cardiol. 1983;51:273-276.
169. Gatzoulis MA, Freeman MA, Siu SC et al. Atrial arrhythmia after surgical closure of atrial septal defects in adults. N Engl J Med. 1999;340:839-846.
170. Medeiros A, Iturralde P, Marquez M et al. [Permanent rhythm and conduction disorders in patients surgically treated for atrial septal defect]. Arch Inst Cardiol Mex. 2000;70:46-54.

171. Kirsh JA, Walsh EP, Triedman JK. Prevalence of and risk factors for atrial fibrillation and intra-atrial re-entrant tachycardia among patients with congenital heart disease. Am J Cardiol. 2002;90:338-340.
172. Triedman JK. Arrhythmias in adults with congenital heart disease Heart. 2002;87:383-389.
173. Reithmann C, Hoffmann E, Dorwarth U et al. Electroanatomical mapping for visualization of atrial activation in patients with incisional atrial tachycardias. European Heart Journal. 2001;22:237-246.
174. Van Hare GF. Electrical-anatomic correlations between typical atrial flutter and intra-atrial re-entry following atrial surgery. J Electrocardiol. 1998;30 Suppl:77-84.
175. Kanter RJ, Garson A, Jr. Atrial arrhythmias during chronic follow-up of surgery for complex congenital heart disease. Pacing Clin Electrophysiol. 1997;20:502-511.
176. Gillette PC, Kugler JD, Garson A, Jr. et al. Mechanisms of cardiac arrhythmias after the Mustard operation for transposition of the great arteries. Am J Cardiol. 1980;45:1225-1230.
177. Vetter VL, Tanner CS, Horowitz LN. Electrophysiologic consequences of the Mustard repair of d-transposition of the great arteries. J Am Coll Cardiol. 1987;10:1265-1273.
178. Kurer CC, Tanner CS, Vetter VL. Electrophysiologic findings after Fontan repair of functional single ventricle. J Am Coll Cardiol. 1991;17:174-181.
179. Birnie D, Tometzki A, Curzio J et al. Outcomes of transposition of the great arteries in the ear of atrial inflow correction. Heart. 1998;80:170-173.
180. Turina M, Siebenmann R, Nussbaumer P et al. Long-term outlook after atrial correction of transposition of great arteries. J Thorac Cardiovasc Surg. 1988;95:828-835.
181. Roos-Hesselink J, Perlroth MG, McGhie J et al. Atrial arrhythmias in adults after repair of tetralogy of Fallot. Correlations with clinical, exercise, and echocardiographic findings. Circulation. 1995;91:2214-2219.
182. Hayes CJ, Gersony WM. Arrhythmias after the Mustard operation for transposition of the great arteries: a long-term study. J Am Coll Cardiol. 1986;7:133-137.
183. Litwin SB, Bhavani SS. The Senning procedure for repair of d-transposition of the great arteries. J Card Surg. 1987;2:415-428.
184. Timmermans C, Rodriguez LM, Reuter D et al. Management of atrial arrhythmias secondary to severe congenital heart disease with the Atrioverter. Pacing Clin Electrophysiol. 2000;23:1181-1183.
185. Balaji S, Johnson TB, Sade RM et al. Management of atrial flutter after the Fontan procedure. J Am Coll Cardiol. 1994;23:1209-1215.
186. Shannon KM. Arrhythmias in Congenital Heart Disease. Curr Treat Options Cardiovasc Med. 1999;1:373-379.
187. Paul T, Trappe HJ, Pfammatter JP et al. [Atrial flutter in young patients after corrective operation of congenital heart defects: therapy by high frequency catheter ablation. Z Kardiol. 1996;85:59-64.
188. Derrick G, Cullen S. Transposition of the Great Arteries Curr Treat Options Cardiovasc Med. 2000;2:499-506.
189. Van Hare GF, Lesh MD, Ross BA et al. Mapping and radiofrequency ablation of intraatrial reentrant tachycardia after the Senning or Mustard procedure for transposition ofthe great arteries. Am J Cardiol. 1996;77:985-991.
190. Dorostkar PC, Cheng J, Scheinman MM. Electroanatomical mapping and ablation of the substrate supporting intraatrial reentrant tachycardia after palliation for complex congenital heart disease. Pacing Clin Electrophysiol. 1998;21:1810-1819.
191. Triedman JK, Bergau DM, Saul JP et al. Efficacy of radiofrequency ablation for control of intraatrial reentrant tachycardia in patients with congenital heart disease J Am Coll Cardiol. 1997;30:1032-1038.
192. Triedman JK, Alexander ME, Love BA et al. Influence of patient factors and ablative technologies on outcomes of radiofrequency ablation of intra-atrial re-entrant tachycardia in patients with congenital heart disease J Am Coll Cardiol. 2002;39:1827-1835.
193. Baker BM, Lindsay BD, Bromberg BI et al. Catheter ablation of clinical intraatrial reentrant tachycardias resulting from previous atrial surgery: localizing and transecting the critical isthmus. J Am Coll Cardiol. 1996;28:411-417.
194. Betts TR, Roberts PR, Allen SA et al. Electrophysiological mapping and ablation of intra-atrial re-entry tachycardia after Fontan surgery with the use of a noncontact mapping system. Circulation. 2000;102:419-425.

195. Van Hare GF, Lesh MD, Stanger P. Radiofrequency catheter ablation of supraventricular arrhythmias in patients with congenital heart disease: results and technical considerations. J Am Coll Cardiol. 1993;22:883-890.
196. Triedman JK, Saul JP, Weindling SN et al. Radiofrequency ablation of intra-atrial reentrant tachycardia after surgical palliation of congenital heart disease. Circulation. 1995;91:707-714.
197. Flinn CJ, Wolff GS, Dick M et al. Cardiac rhythm after the Mustard operation for complete transposition of the great arteries. N Engl J Med. 1984;310:1635-1638.
198. Rhodes LA, Wernovsky G, Keane JF et al. Arrhythmias and intracardiac conduction after the arterial switch operation. J Thorac Cardiovasc Surg. 1995;109:303-310.
199. Konstantinov IE, Alexi-Meskishvili VV. Cavo-pulmonary shunt: from the first experiments to clinical practice. Ann Thorac Surg. 1999;68:1100-1106.
200. Driscoll DJ, Offord KP, Feldt RH et al. Five- to fifteen-year follow-up after Fontan operation. Circulation. 1992;85:469-496.
201. Fishberger SB, Wernovsky G, Gentles TL et al. Factors that influence the development of atrial flutter after the Fontan operation. J Thorac Cardiovasc Surg. 1997;113:80-86.
202. Cecchin F, Johnsrude CL, Perry JC et al. Effect of age and surgical technique on symptomatic arrhythmias after the Fontan procedure. Am J Cardiol. 1995;76:386-391.
203. Agnoletti G, Borghi A, Vignati G et al. Fontan conversion to total cavopulmonary connection and arrhythmia ablation: clinical and functional results Heart. 2003;89:193-198.
204. Gelatt M, Hamilton RM, McCrindle BW et al. Risk factors for atrial tachyarrhythmias after the Fontan operation. J Am Coll Cardiol. 1994;24:1735-1741.
205. Mavroudis C, Deal BJ, Backer CL. Arrhythmia surgery in association with complex congenital heart repairs excluding patients with fontan conversion Semin Thorac Cardiovasc Surg Pediatr Card Surg Annu. 2003;6:33-50.
206. Balaji S, Gewillig M, Bull C et al. Arrhythmias after the Fontan procedure. Comparison of total cavopulmonary connection and atriopulmonary connection. Circulation. 1991;84:III162-III167.
207. Bink-Boelkens MT, Meuzelaar KJ, Eygelaar A. Arrhythmias after repair of secundum atrial septal defect: the influence of surgical modification. Am Heart J. 1988;115:629-633.
208. Morton JB, Sanders P, Vohra JK et al. Effect of chronic right atrial stretch on atrial electrical remodeling in patients with an atrial septal defect. Circulation. 2003;107:1775-1782.
209. Dietl CA, Cazzaniga ME, Dubner SJ et al. Life-threatening arrhythmias and RV dysfunction after surgical repair of tetralogy of Fallot. Comparison between transventricular and transatrial approaches. Circulation. 1994;90:II7-12
210. Harrison DA, Siu SC, Hussain F et al. Sustained atrial arrhythmias in adults late after repair of tetralogy of fallot. Am J Cardiol. 2001;87:584-588.
211. Gatzoulis MA, Balaji S, Webber SA et al. Risk factors for arrhythmia and sudden cardiac death late after repair of tetralogy of Fallot: a multicentre study. Lancet. 2000;356:975-981.